CERN-EP-2017-252
2018/02/23

CMS-SUS-17-001

Search for top squarks and dark matter particles in opposite-charge dilepton final states at $\sqrt{s} = 13\,\text{TeV}$

The CMS Collaboration*

Abstract

A search for new physics is presented in final states with two oppositely charged leptons (electrons or muons), jets identified as originating from b quarks, and missing transverse momentum ($p_{\mathrm{T}}^{\mathrm{miss}}$). The search uses proton-proton collision data at $\sqrt{s} = 13\,\text{TeV}$ amounting to $35.9\,\text{fb}^{-1}$ of integrated luminosity collected using the CMS detector in 2016. Hypothetical signal events are efficiently separated from the dominant $\mathrm{t\bar{t}}$ background with requirements on $p_{\mathrm{T}}^{\mathrm{miss}}$ and transverse mass variables. No significant deviation is observed from the expected background. Exclusion limits are set in the context of simplified supersymmetric models with pair-produced top squarks. For top squarks, decaying exclusively to a top quark and a neutralino, exclusion limits are placed at 95% confidence level on the mass of the lightest top squark up to 800 GeV and on the lightest neutralino up to 360 GeV. These results, combined with searches in the single-lepton and all-jet final states, raise the exclusion limits up to 1050 GeV for the lightest top squark and up to 500 GeV for the lightest neutralino. For top squarks undergoing a cascade decay through charginos and sleptons, the mass limits reach up to 1300 GeV for top squarks and up to 800 GeV for the lightest neutralino. The results are also interpreted in a simplified model with a dark matter (DM) particle coupled to the top quark through a scalar or pseudoscalar mediator. For light DM, mediator masses up to 100 (50) GeV are excluded for scalar (pseudoscalar) mediators. The result for the scalar mediator achieves some of the most stringent limits to date in this model.

Published in Physical Review D as doi:10.1103/PhysRevD.97.032009.

*See Appendix A for the list of collaboration members

1 Introduction

The top quark couples to the Higgs boson more strongly than other fermions because of its large mass. As a result, it plays a prominent role in the so-called hierarchy problem [1, 2] of the standard model (SM) of particle physics, since its dominant contribution in the loop corrections to the Higgs boson mass exposes the theory to higher energy scales present in nature. Supersymmetry (SUSY) [3–10] is a well-motivated theory beyond the SM that provides a solution to the hierarchy problem. In addition, in R-parity conserving SUSY [11], the lightest SUSY particle (LSP) is stable and can be a viable dark matter (DM) candidate, assuming it is neutral and weakly interacting. Presently, the lighter SUSY particles may have masses in the TeV range and therefore could be produced in proton-proton (pp) collisions at the CERN LHC. The scalar partners of the right- and left-handed top quarks, the top squarks $\widetilde{\mathrm{t}}_R$ and $\widetilde{\mathrm{t}}_L$, can be among these particles. These two states mix into the mass eigenstates $\widetilde{\mathrm{t}}_1$ and $\widetilde{\mathrm{t}}_2$. The lighter one, $\widetilde{\mathrm{t}}_1$, could be within the LHC energy reach to provide a natural solution to the hierarchy problem [12], which strongly motivates searches for top squark production.

In this paper, we present a search for top squark pair production in a final state with two leptons (electrons or muons), hadronic jets identified as originating from b quarks, and significant transverse momentum imbalance. The search is performed using data from pp collisions collected with the CMS detector at the LHC during 2016 at a center-of-mass energy of 13 TeV, corresponding to an integrated luminosity of $35.9\,\mathrm{fb}^{-1}$. We employ an efficient background reduction strategy that suppresses the large background from SM $\mathrm{t\bar{t}}$ events by several orders of magnitude through use of dedicated transverse-mass variables [13, 14]. The predicted SM backgrounds in the various search regions are validated in data control samples orthogonal in selection to the signal regions in data.

The search is interpreted in simplified models [15–17] describing the strong production of pairs of top squarks. We consider different decay modes, following the naming convention in Ref. [18]. In the T2tt model (Fig. 1, upper left), each top squark decays into a top quark and the lightest neutralino $\widetilde{\chi}_1^0$, which is the LSP. Alternatively, we consider the T2bW model (Fig. 1, upper right), where both top squarks decay into a b quark and an intermediate chargino ($\widetilde{\chi}_1^{\pm}$) which further decays into a W boson and an LSP. In both models, leptonic decays of the two W bosons provide a low-background final state with two oppositely charged leptons, jets from b quarks, and significant transverse momentum imbalance due to undetected LSPs and neutrinos. The obtained results are then combined with results from searches in the same dataset in the single-lepton and all-jet final states [19, 20]. Finally, we consider for the first time the T8bb$\ell\ell\nu\nu$ model (Fig. 1, lower left), where both top squarks decay via charginos to sleptons and, subsequently, to neutralinos leading to a final state with the same particle content as in the T2tt model. Here, sleptons are the SUSY partners of leptons, and the branching fraction of the chargino is taken to be identical for all three flavors. In this way, and contrary to the T2tt and T2bW models, the branching fraction to a pair of oppositely charged leptons is 100% when decays to τ leptons are included. Searches based on T2tt and T2bW models using 8 and 13 TeV pp collision data recorded before 2016 were published by the CMS [21–23] and the ATLAS [24–28] experiments, with a $\widetilde{\mathrm{t}}_1$ mass excluded up to 700 GeV in the T2tt model.

As an alternative to the SUSY hypothesis, we also interpret the search in a simplified model where a DM candidate χ interacts with SM particles through a scalar (ϕ) or pseudoscalar (a) mediator [29–33]. Assuming minimal flavor violation [34, 35], the DM particles are dominantly produced in pairs in association with a $\mathrm{t\bar{t}}$ pair (Fig. 1, lower right). This model predicts therefore the same final state as considered in SUSY phenomenology, with the transverse momentum imbalance provided by the DM particles. Prior searches for such direct DM production via

scalar and pseudoscalar mediators have been carried out at the LHC with 8 TeV data [36, 37], and more recently with 13 TeV data [38–40].

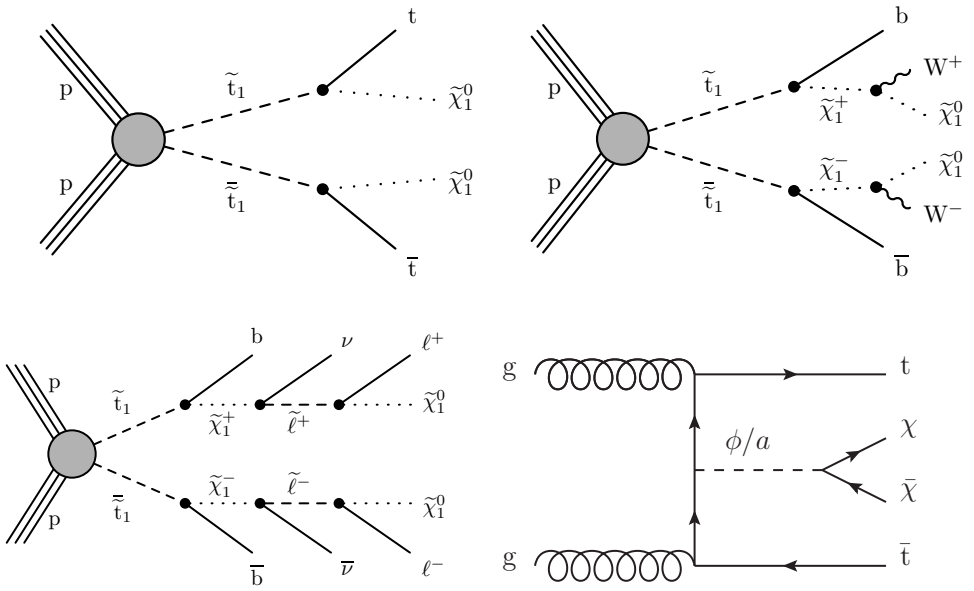

Figure 1: Diagrams for simplified SUSY models and for direct DM production: strong production of top squark pairs $\tilde{t}_1\bar{\tilde{t}}_1$, where each top squark decays to a top quark and a $\tilde{\chi}_1^0$ (T2tt model, upper left), or where each top squark decays into a b quark and an intermediate $\tilde{\chi}_1^\pm$ that further decays into a W boson and a $\tilde{\chi}_1^0$ (T2bW model, upper right), or to a neutrino and an intermediate slepton $\nu\tilde{\ell}^\pm$ that yield $\nu\tilde{\chi}_1^0$ and an $\ell^\pm$ from the virtual slepton decay (T8bb$\ell\ell\nu\nu$ model, lower left). Direct DM production through scalar or pseudoscalar mediators in association with top quarks is shown at the lower right.

2 The CMS detector

The central feature of the CMS detector is a superconducting solenoid of 6 m internal diameter, providing a magnetic field of 3.8 T. A silicon pixel and a silicon strip tracker, a lead tungstate crystal electromagnetic calorimeter (ECAL), and a brass and scintillator hadron calorimeter, each comprising a barrel and two end sections reside within the solenoid volume. Muons are measured in gas-ionization detectors embedded in the magnet steel flux-return yoke outside the solenoid. Extensive forward calorimetry complements the coverage provided by the barrel and endcap detectors that improve the measurement of the imbalance in transverse momentum. A more detailed description of the CMS detector, together with a definition of the coordinate system and the kinematic variables, can be found in Ref. [41].

3 Event samples

During data taking, events are selected for offline analysis by different trigger algorithms that require the presence of one or two leptons (electrons or muons). For the dilepton triggers, which accept the majority of events with two leptons, the thresholds are 23 GeV on the leading lepton p_T and 12 GeV (electron) or 8 GeV (muon) on the subleading lepton p_T. Efficiencies of the dilepton triggers are measured in data events that are selected independently of the leptons, based on the presence of jets and requirements on the transverse momentum imbalance (p_T^{miss}).

Typical values range from 95 to 99%, depending on the momenta and pseudorapidities (η) of the two leptons and are applied as scale factors to simulated events.

The top quark antiquark pair production ($\mathrm{t\bar{t}}$) and t-channel single top quark background samples are simulated using the POWHEG v2 [42, 43] event generator, and are normalized to next-to-next-to-leading order (NNLO) cross sections [44–50]. Events with single top quarks produced in association with W bosons (tW) are simulated using POWHEG v1 [51] and normalized to the NNLO cross section. Drell–Yan and $\mathrm{t\bar{t}Z}$ events are generated with MADGRAPH5_aMC@NLO v2.2.2 [52] at leading order (LO) and next-to-leading order (NLO), respectively, and their cross sections are computed at NNLO [53] and NLO [54], respectively. The processes $\mathrm{t\bar{t}W}$, tZq, $\mathrm{t\bar{t}}\gamma$, and the triboson processes are generated using MADGRAPH5_aMC@NLO at NLO, while tWZ is generated at LO. The diboson and $\mathrm{t\bar{t}H}$ processes are generated using POWHEG v2 at NLO. These processes are normalized to the most precise available cross section, corresponding to NLO accuracy in most cases.

Generated events are interfaced with PYTHIA v8.205 [55] using the CUETP8M1 tune [56, 57] or, for $\mathrm{t\bar{t}}$ and $\mathrm{t\bar{t}H}$ backgrounds, the CUETP8M2 tune, to simulate parton showering, hadronization, and the underlying event. The NNPDF3.0 [58] parton distribution functions (PDFs) at NLO and LO are used consistently with NLO and LO event generators, respectively. The events are subsequently processed with a GEANT4-based simulation model [59] of the CMS detector.

Signal samples including top squark pairs are generated with MADGRAPH5_aMC@NLO at LO precision, interfaced with PYTHIA. For the T2tt and T2bW models, the top squark mass is varied from 150 to 1200 GeV and the mass of the LSP is scanned from 1 to 650 GeV. The mass of the chargino in the T2bW model is assumed to be equal to the mean of the masses of the top squark and the lightest neutralino. For the T8bb$\ell\ell\nu\nu$ model, we vary the top squark mass between 200 to 1400 GeV and the mass of the LSP from 1 to 1000 GeV. The masses of the intermediate chargino and slepton states in the T8bb$\ell\ell\nu\nu$ model are chosen as follows: for the chargino mass we assume $m_{\tilde{\chi}_1^+} = (m_{\tilde{\mathrm{t}}_1} + m_{\tilde{\chi}_1^0})/2$, while the slepton masses are chosen by the three values $x = 0.95$, 0.50, 0.05 in $m_{\tilde{\ell}} = x\,(m_{\tilde{\chi}_1^+} - m_{\tilde{\chi}_1^0}) + m_{\tilde{\chi}_1^0}$. The signal production cross sections are normalized to NLO plus next-to-leading logarithmic (NLL) accuracy [60]. Simulation of the detector response is performed using the CMS fast detector simulation [61].

For the simplified model of $\mathrm{t\bar{t}}$+DM production, MADGRAPH5_aMC@NLO is used at LO to generate events with at most one additional parton from initial-state radiation. We follow the recommendations from Ref. [33]: the DM particle is taken to be a Dirac fermion, while the spin-0 mediator can have either scalar or pseudoscalar couplings to both quarks and DM, ignoring mixing with the SM Higgs boson in the scalar case. Yukawa couplings proportional to $g_{\mathrm{q}} m_{\mathrm{q}}$ are assumed between the mediator and the quarks of mass m_{q}, where the coupling strength g_{q} is taken to be 1 and assumed to be flavor universal. The coupling strength g_{DM} of the mediator to the DM particles is also set to 1. The aforementioned GEANT4-based detector simulation is used for this signal.

All simulated samples include the simulation of so-called pileup from the presence of additional pp collisions in simultaneous or preceding bunch crossings, and are reweighted according to the distribution of the true number of interactions in the main collision's bunch crossing.

4 Object selection

Offline event reconstruction uses the CMS particle-flow (PF) algorithm [62], yielding a consistent set of electron [63], muon [64], charged and neutral hadron, and photon candidates.

These particles are defined with respect to the primary pp interaction vertex, chosen to have the largest value of summed physics-object p_T^2, where these physics objects are reconstructed by a jet finding algorithm [65, 66] applied to all charged tracks associated with the vertex.

Electron candidates are reconstructed using tracking and ECAL information, by combining the clusters of energy deposits in the ECAL with Gaussian sum filter tracks [63]. The electron identification is performed using shower shape variables, track-cluster matching variables, and track quality variables. The selection is optimized to identify electrons from the decay of SM bosons with a 70% efficiency while rejecting electron candidates originating from jets. To reject electrons originating from photon conversion inside the detector, electrons are required to have all possible hits in the innermost tracker layers and to be incompatible with any conversion-like secondary vertices. Identification of muon candidates is performed using the quality of the geometrical matching between the measurements of the tracker and the muon system [64].

All lepton candidates are required to satisfy $p_T > 25(20)$ GeV for the leading (subleading) lepton and $|\eta| < 2.4$. Consistency of the lepton track with the selected primary vertex is enforced by vetoing lepton candidates whose tracks have a significance of the transverse impact parameter above 4. Here, the impact parameter is the minimum three-dimensional distance between the lepton trajectory and the primary vertex. Its significance is defined as the ratio of the impact parameter to its uncertainty. The longitudinal displacement from the primary collision vertex must also be less than 0.1 cm.

Lepton candidates are required to be isolated. For each candidate a cone with radius $\Delta R = \sqrt{(\Delta\eta)^2 + (\Delta\phi)^2} = 0.3$ (where ϕ is azimuthal angle in radians) around the track direction at the event vertex is constructed. The relative isolation ($I_{\text{rel, 0.3}}$) is defined as the scalar p_T sum, normalized to the lepton p_T, of photons and neutral and charged hadrons reconstructed by the PF algorithm within this cone. In order to reduce dependence on the number of pileup interactions, charged hadron candidates are included in the sum only if they are consistent with originating from the selected primary vertex in the event. The contribution of neutral particles from pileup events is estimated following the method described in Ref. [63], and subtracted from the isolation sum. For a lepton candidate to be isolated, $I_{\text{rel, 0.3}}$ has to be smaller than 0.12.

Jets are clustered from PF candidates using the anti-k_T algorithm [65] with a distance parameter of $R = 0.4$. The influence of pileup is mitigated using the charged hadron subtraction technique, by subtracting the energy of charged hadrons associated to vertices other than the primary vertex. Jet momenta are then further calibrated, accounting for deposits from neutral pileup particles and the imperfect detector response [67], and quality criteria are applied for jets with $p_T > 30$ GeV and $|\eta| < 2.4$. To arbitrate between jets and leptons, jets that are found within a cone with radius $\Delta R = 0.4$ around any isolated lepton are removed from the set of selected jets. The scalar p_T sum of the jets that pass this selection is denoted by H_T.

The vector $\vec{p}_T^{\,\text{miss}}$ is defined as the negative vector p_T sum of all PF candidates reconstructed in an event and is corrected to account for the jet energy corrections. Its magnitude is denoted by p_T^{miss}. Events with possible contributions from beam halo processes or anomalous noise in the calorimeter are rejected using dedicated filters [68].

A multivariate b tagging discriminator CSVv2 [69] is used to identify jets that originate from a b quark (b jets). The chosen "medium" working point has a mistag rate of approximately 1% for light flavor jets and a corresponding b tagging efficiency of 55% to 65% depending on jet transverse momentum and pseudorapidity [69].

Scale factors are applied in simulation to take into account the differences of lepton reconstruction, identification and isolation as well as b tagging efficiencies in data and simulation. Typical

corrections are less than 1% per lepton and less than 10% per b-tagged jet.

5 Search strategy

We select events containing a pair of leptons with opposite charge, and we require the invariant mass of the lepton pair to be greater than 20 GeV, to suppress backgrounds with misidentified or nonprompt leptons from the hadronization of (heavy flavor) jets in multijet events. Events with additional leptons with $p_T > 15$ GeV and satisfying a looser isolation criterion of $I_{\text{rel, 0.3}} < 0.4$ are vetoed. In case of a same-flavor (SF) lepton pair, we suppress contributions from SM Drell–Yan production with a requirement on the dilepton mass, $|m_Z - m(\ell\ell)| > 15$ GeV, where $m(\ell\ell)$ is the invariant mass of the dilepton system and m_Z is the mass of the Z boson. To further suppress this and other vector boson backgrounds, we require the number of jets (N_{jets}) to be at least two and, among them, the number of b jets ($N_{\text{b jets}}$) to be at least one. After additionally requiring $p_T^{\text{miss}} > 80$ GeV, a small background remains from events with vector bosons and highly energetic jets that are severely mismeasured. We further reduce this background by defining $S = p_T^{\text{miss}}/\sqrt{H_T}$ and requiring $S > 5\,\text{GeV}^{1/2}$ and, furthermore, by placing a requirement on the angular separation of $\vec{p}_T^{\text{miss}}$ and the momenta of the leading (j_1) and subleading (j_2) jets in the azimuthal plane. The selection above is summarized in Table 1 and defines the event sample, which is dominated by events with top quark pairs that decay to a dilepton final state.

Table 1: Overview of the preselection requirements.

Leptons	= 2 (e or μ), oppositely charged
$m(\ell\ell)$	>20 GeV
$\lvert m_Z - m(\ell\ell)\rvert$	>15 GeV, same flavor only
N_{jets}	$\geq$2
$N_{\text{b jets}}$	$\geq$1
p_T^{miss}	>80 GeV
S	>5 GeV $^{1/2}$
$\cos\Delta\phi(p_T^{\text{miss}}, j_1)$	<0.80
$\cos\Delta\phi(p_T^{\text{miss}}, j_2)$	<0.96

The main search variable in this analysis is

$$M_{T2}(\ell\ell) = \min_{\vec{p}_T^{\,\text{miss}1} + \vec{p}_T^{\,\text{miss}2} = \vec{p}_T^{\,\text{miss}}} \left(\max \left[M_T(\vec{p}_T^{\,\text{vis}1}, \vec{p}_T^{\,\text{miss}1}), M_T(\vec{p}_T^{\,\text{vis}2}, \vec{p}_T^{\,\text{miss}2}) \right] \right), \tag{1}$$

where the choice $\vec{p}_T^{\,\text{vis}1,2} = \vec{p}_T^{\,\ell 1,2}$ corresponds to the definition introduced in Ref. [70] and used in Ref. [22]. The calculation of $M_{T2}(\ell\ell)$ is performed through the algorithm discussed in Ref. [71] assuming vanishing mass for the undetected particles. Under the hypothesis of a well-reconstructed dileptonic $\mathrm{t\bar{t}}$ or WW event, the minimization in Eq. 1 encompasses the correct neutrino momenta, and thus $M_{T2}(\ell\ell)$ has an endpoint at the parent particle's mass [14], here m_W. When the azimuthal angle of $\vec{p}_T^{\,\text{miss}}$ falls within the smaller of the two opening angles defined by the leptons in the transverse plane, it follows that $M_{T2}(\ell\ell)$ vanishes because the minimization procedure will find a partitioning where $\vec{p}_T^{\,\text{miss}1,2}$ and $\vec{p}_T^{\,\ell 1,2}$ are both parallel.

The key feature of this analysis is that the presence of additional invisible particles, e.g., the LSP $\tilde{\chi}_1^0$ or the DM particle χ, breaks the correlation between the $\vec{p}_T^{\,\text{miss}}$ and the lepton transverse momenta that define the $M_{T2}(\ell\ell)$ endpoint. Hence, we expect the events predicted by the diagrams depicted in Fig. 1 to populate the tails of this distribution. The distribution of $M_{T2}(\ell\ell)$ in

simulation after the preselection is shown in Fig. 2 (left) for $M_{T2}(\ell\ell) > 100\,\text{GeV}$ and including a T2tt signal with a mass configuration with $m_{\tilde{t}} = 750\,\text{GeV}$ and $m_{\tilde{\chi}_1^0} = 1\,\text{GeV}$, as well as a more compressed signal scenario with $m_{\tilde{t}} = 600\,\text{GeV}$ and $m_{\tilde{\chi}_1^0} = 300\,\text{GeV}$.

We refine the analysis by using two more observables to define signal regions, $M_{T2}(b\ell b\ell)$ and p_T^{miss}. For $M_{T2}(b\ell b\ell)$, we choose [70] $\vec{p}_T^{\,\text{vis1,2}} = \vec{p}_T^{\,\text{b1,2}} + \vec{p}_T^{\,\ell 1,2}$, which requires two b-tagged jets. If only one b tagged jet is found in the event, the jet with the highest p_T that does not pass the b tagging selection is taken instead. The ambiguity when pairing leptons with b jets for $M_{T2}(b\ell b\ell)$ is resolved by selecting the configuration which minimizes the maximum invariant mass of the two lepton-jet pairs. Similar to the procedure to obtain $M_{T2}(\ell\ell)$, we break up $\vec{p}_T^{\,\text{miss}}$ into two parts and pair them with $\vec{p}_T^{\,\text{vis1,2}}$ in order to define M_T, and then compute $M_{T2}(b\ell b\ell)$ analogously to Eq. (1). For dileptonic $t\bar{t}$ events, $M_{T2}(b\ell b\ell)$ has an endpoint at the top quark mass. After a tight threshold of $M_{T2}(\ell\ell) > 100\,\text{GeV}$, both $M_{T2}(b\ell b\ell)$ and p_T^{miss} still exhibit significant discrimination power. This is shown in Fig. 2 (middle) for $M_{T2}(b\ell b\ell)$ and Fig. 2 (right) for p_T^{miss}.

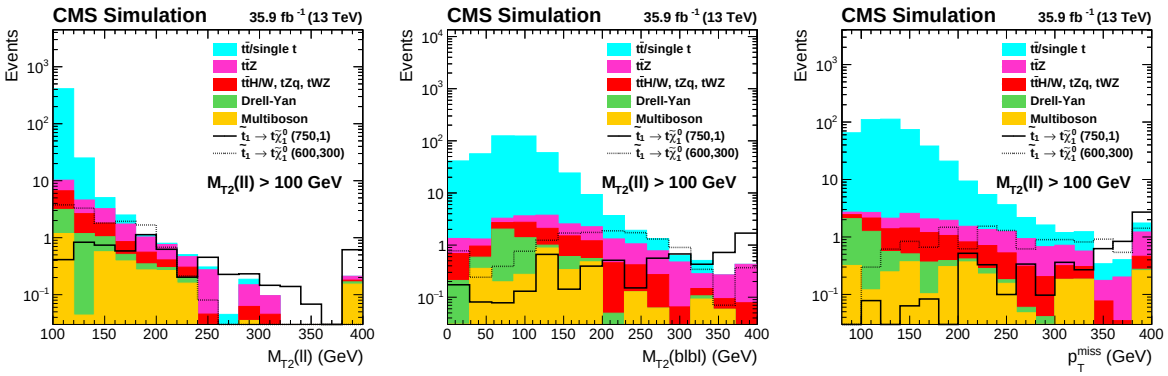

Figure 2: Distributions of $M_{T2}(\ell\ell)$ (left), $M_{T2}(b\ell b\ell)$ (center), and p_T^{miss} (right) in simulation after preselection and requiring $M_{T2}(\ell\ell) > 100\,\text{GeV}$. A T2tt signal is shown with masses $m_{\tilde{t}} = 750\,\text{GeV}$ and $m_{\tilde{\chi}_1^0} = 1\,\text{GeV}$, as well as a more compressed signal with $m_{\tilde{t}} = 600\,\text{GeV}$ and $m_{\tilde{\chi}_1^0} = 300\,\text{GeV}$.

Based on sensitivity studies for a wide range of signal scenarios, the signal regions listed in Table 2 are chosen. These regions are further split depending on the flavor of the leptons into different- and same-flavor signal regions. There is no overlap among the signal regions themselves or with background enriched regions (control regions) used in the following.

Table 2: Definition of the signal regions. The regions are further split into different- and same-flavor regions.

$M_{T2}(b\ell b\ell)$ (GeV)	p_T^{miss} (GeV)	$100 < M_{T2}(\ell\ell) < 140\,\text{GeV}$	$140 < M_{T2}(\ell\ell) < 240\,\text{GeV}$	$M_{T2}(\ell\ell) > 240\,\text{GeV}$
0–100	80–200	SR0	SR6	SR12
	>200	SR1	SR7	
100–200	80–200	SR2	SR8	
	>200	SR3	SR9	
>200	80–200	SR4	SR10	
	>200	SR5	SR11	

6 Background predictions

The major backgrounds from SM processes in the search regions after the event selection are single top quark and top quark pair events with either severely mismeasured p_T^{miss} or misiden-

tified leptons. Smaller contributions come from the same processes in association with a Z, W, or an H boson ($t\bar{t}Z$, $t\bar{t}W$, $t\bar{t}H$, tqZ) and Drell–Yan and multiboson production (WW, WZ, ZZ, WWW, WWZ, WZZ, and ZZZ). In the following, we discuss the estimation of these different background components.

6.1 Top quark background

Events containing single or pair-produced top quarks populate low regions in the distributions of the three analysis variables $M_{\mathrm{T2}}(\ell\ell)$, $M_{\mathrm{T2}}(\mathrm{b}\ell\mathrm{b}\ell)$, and $p_{\mathrm{T}}^{\mathrm{miss}}$ if the momenta in the events are well measured. Studies based on simulation show two main sources of top quark background in the signal regions. First, a severe mismeasurement of jet energy caused by the loss of photons and neutral hadrons showering in masked channels of the calorimeters can induce large $p_{\mathrm{T}}^{\mathrm{miss}}$ mismeasurement and promote an otherwise well-measured event to the signal regions. Additionally, neutrinos with high p_{T} within jets cause mismeasurements of the jet p_{T}. A control region requiring same-flavor leptons satisfying $|m(\ell\ell) - m_{\mathrm{Z}}| < 15\,\mathrm{GeV}$ is used to constrain any mismodeling of this rare effect by comparing the $p_{\mathrm{T}}^{\mathrm{miss}}$ tail between data and simulation. It is found that the simulation predicts well such mismeasurements, and no sign of unaccounted effects in the $p_{\mathrm{T}}^{\mathrm{miss}}$ measurement is observed. Furthermore, the modeling of the tail of the analysis variable distributions is validated in control regions that invert the requirement on one or more of the following variables: $p_{\mathrm{T}}^{\mathrm{miss}}$ with no requirement on S, $N_{\mathrm{b\,jets}}$, and N_{jets}. As an example, Fig. 3 (left) shows the $M_{\mathrm{T2}}(\ell\ell)$ distribution in the different-flavor channel with $N_{\mathrm{b\,jets}} \geq 1$, $N_{\mathrm{jets}} \geq 2$, $p_{\mathrm{T}}^{\mathrm{miss}} < 80\,\mathrm{GeV}$, and no requirement on S. No significant sign of mismodeling is found in any of the control regions over at least three orders of magnitude in event yields. The uncertainties from experimental effects, as described in Section 7, are shown with a hatched band.

Second, an electron or muon may fail the identification requirements, or the event may have a τ lepton produced in a W boson decay. If there is a nonprompt lepton from the hadronization of a b quark or a charged hadron misidentified as a lepton selected in the same event, the reconstructed value for $M_{\mathrm{T2}}(\ell\ell)$ is not bound by the W mass. To validate the modeling of this contribution, we select events with one additional lepton satisfying loose isolation requirements on top of the selection in Table 1. In order to mimic the lost prompt lepton background, we recompute $M_{\mathrm{T2}}(\ell\ell)$ by combining each of the isolated leptons with the extra lepton in both data and simulation. Since the transverse momentum balance is not significantly changed by lepton misidentification, the $p_{\mathrm{T}}^{\mathrm{miss}}$ observable is not modified. The resulting $M_{\mathrm{T2}}(\ell\ell)$ distribution is shown in Fig. 3 (right) and serves as a validation of the modeling of the lost lepton background. We observe overall good agreement between simulation and data, indicating that simulation describes such backgrounds well.

Top quark backgrounds are split into three categories in the signal regions and uncertainties related to them are assigned based on the agreement of data and simulation in the studies above. The first category consists of events which are promoted to the $M_{\mathrm{T2}}(\ell\ell)$ tail due to Gaussian jet energy mismeasurements within approximately twice the jet energy resolution. It comprises 25–55% of the top quark background, depending on the signal region, and we assign a 15% uncertainty in the yield of this fraction. The second category, 40–50% of the total top quark background yield, contains events with jets with more severe energy mismeasurements. A 30% uncertainty, based on studies in control regions, is assigned to the yield of events. Events containing misidentified electrons or muons constitute 1–25% of the top quark background, and based on studies on the modeling of the misidentification rate, a 50% uncertainty is assigned. Finally, we proceed to predict the background from single top and top quark pair production by normalizing simulated distributions to the number of events in a data region defined by

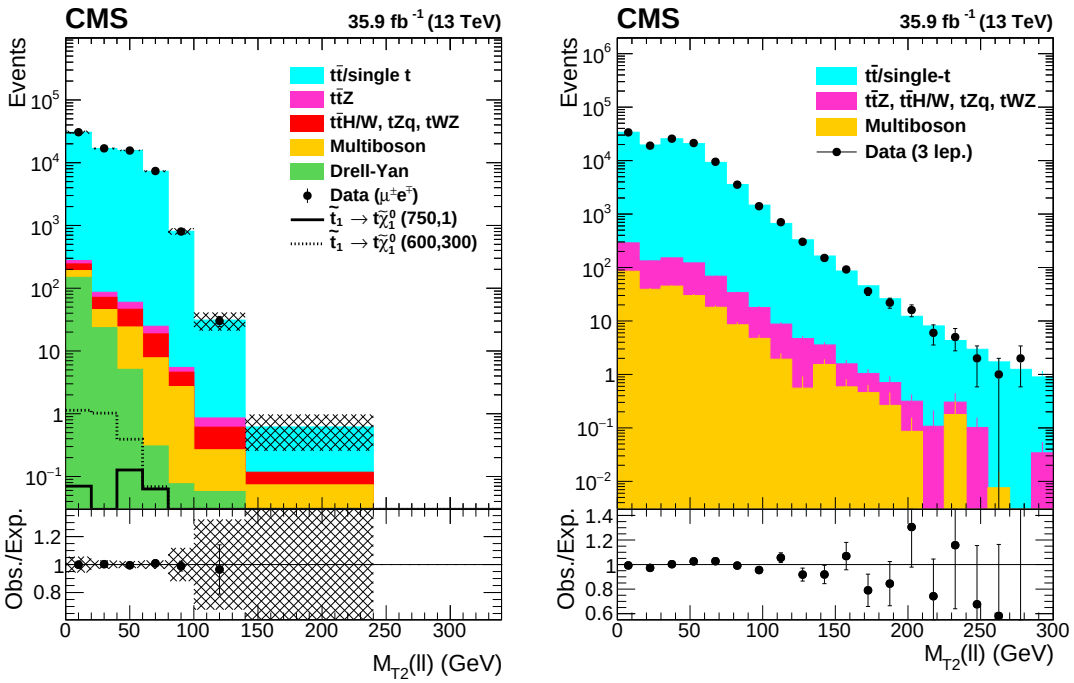

Figure 3: Left: distribution of $M_{\mathrm{T2}}(\ell\ell)$ in a control region enriched in $\mathrm{t\bar{t}}$ events and defined by $N_{\text{jets}} \geq 2$, $N_{\text{b jets}} \geq 1$, and $p_{\mathrm{T}}^{\text{miss}} < 80\,\text{GeV}$. The hatched band shows the uncertainties from experimental effects, as described in Section 7. Right: distribution of $M_{\mathrm{T2}}(\ell\ell)$ after swapping an isolated lepton with an additional non-isolated lepton, as described in the text. For both plots, simulated yields are normalized to data using the yields in the $M_{\mathrm{T2}}(\ell\ell) < 100\,\text{GeV}$ region.

the selection in Table 1 and an additional requirement of $M_{T2}(\ell\ell) < 100\,\text{GeV}$. In this way, experimental uncertainties affecting the overall normalization are largely reduced.

6.2 Top quark + X background

Top quarks produced in association with a boson ($t\bar{t}Z$, $t\bar{t}W$, $t\bar{t}H$, tqZ) form an irreducible background in decay channels where the bosons decay to leptons or neutrinos. Among these, the $t\bar{t}Z$ background, with $Z \to \nu\bar{\nu}$ providing extra genuine p_T^{miss}, is the dominant one. The overall normalization of this contribution is measured in the decay mode

$$t\bar{t}Z \to (t \to b\ell^{\pm}\nu)(t \to bjj)(Z \to \ell^{\pm}\ell^{\mp})$$

in control regions with exactly three leptons ($\mu\mu\mu$, $\mu\mu e$, μee and eee), where the leading, subleading, and trailing lepton transverse momentum are required to satisfy thresholds of 40, 20, and 10 GeV, respectively. All pairs of same-flavor leptons with opposite charge are required to satisfy $|m(\ell\ell) - m_Z < 10\,\text{GeV}|$. Five control regions requiring different N_{jets} and $N_{\text{b jets}}$ combinations are defined. The simulated number of $t\bar{t}Z$ events is fitted to the number of observed events in these regions. The normalizations of other background components are allowed to vary within their uncertainties, and the values returned by the fit are consistent with the initial ones. The number of events in the control regions in simulation and data is shown in Fig. 4 before (left) and after (right) the fit. Including systematic uncertainties, the fit yields a scale factor of 1.09 ± 0.15, which is then used to normalize the $t\bar{t}Z$ background in the signal regions. The scale factor uncertainty is fully accounted for in the background prediction.

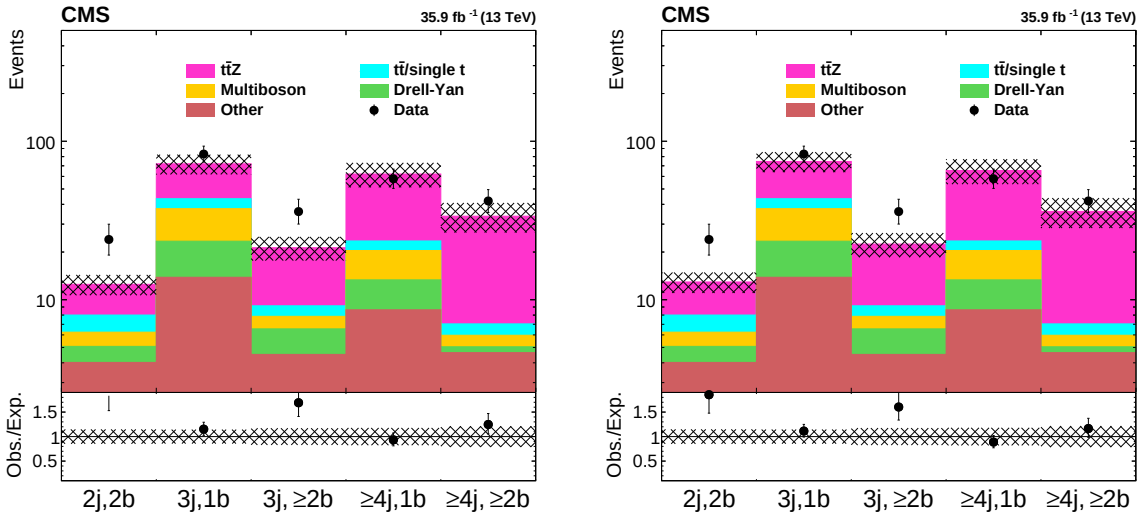

Figure 4: Expected and observed yields in the five $t\bar{t}Z$ control regions, which are defined by different requirements on the number of reconstructed jets and b jets, before (left) and after the fit (right). The hatched band contains all uncertainties discussed in the text.

Furthermore, we constrain a potential mismodeling of the $M_{T2}(\ell\ell)$ and p_T^{miss} distributions for the $t\bar{t}Z$ (with $Z \to \nu\bar{\nu}$) background in a data control sample dominated by $t\bar{t}\gamma$ events, using the photon as a proxy for the Z boson and adding its momentum to the p_T^{miss}. To mitigate the difference between the massive Z boson and the massless photon, the simulated photon momentum is reweighted to match the distribution of the Z boson momentum. After this procedure, we find good agreement between the simulated $t\bar{t}\gamma$ and $t\bar{t}Z$ distributions. Repeating the exercise on data, we find agreement within the statistical precision and assign a conservative additional uncertainty of 20%.

6.3 Drell–Yan and multiboson backgrounds

Drell–Yan events constitute only a small background component after the analysis selection. In order to measure the residual contribution, we select dilepton events where we invert the Z boson veto, the b jet requirements, and the angular separation requirements on jets and $\vec{p}_{\mathrm{T}}^{\,\mathrm{miss}}$. From simulation, this selection is expected to retain about 85% Drell–Yan events, while the subleading contribution comes from multiboson events. For each same-flavor signal region, we define a corresponding control region with the selections above and the signal region requirements on $M_{\mathrm{T2}}(\ell\ell)$, $M_{\mathrm{T2}}(\mathrm{b}\ell\mathrm{b}\ell)$, and $p_{\mathrm{T}}^{\mathrm{miss}}$.

Including systematic uncertainties, we perform a likelihood fit of the predicted yields in these control regions and extract simulation-to-data scale factors that amount to 1.31 ± 0.19 for the Drell–Yan background and 1.19 ± 0.17 for the multiboson background component. The $M_{\mathrm{T2}}(\ell\ell)$ distribution with this selection is presented in Fig. 5 (left) after applying the overall scale factors. The fit procedure is sensitive to the Drell–Yan and multiboson contributions separately, because their $M_{\mathrm{T2}}(\mathrm{b}\ell\mathrm{b}\ell)$ and $p_{\mathrm{T}}^{\mathrm{miss}}$ distributions differ substantially, as shown in Fig. 5 (middle) and (right), respectively. Good agreement between the prediction and observation of both Drell–Yan and multiboson contributions is observed, and the result in all 13 control regions is shown in Fig. 6.

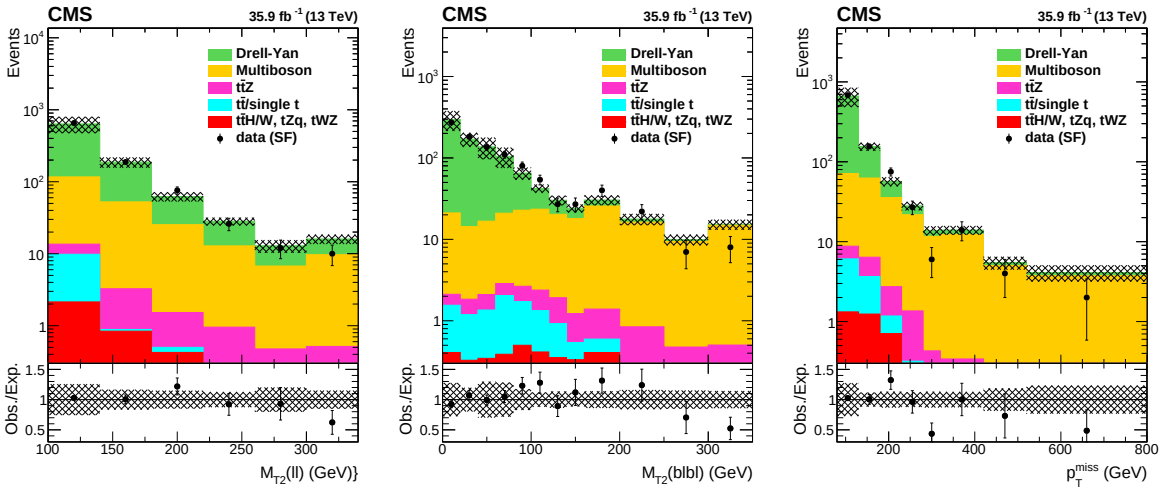

Figure 5: Distributions of $M_{\mathrm{T2}}(\ell\ell)$ (left), $M_{\mathrm{T2}}(\mathrm{b}\ell\mathrm{b}\ell)$ (center), and $p_{\mathrm{T}}^{\mathrm{miss}}$ (right) for SF events falling within the Z boson mass window ($|m(\ell\ell) - m_{\mathrm{Z}}| < 15\,\mathrm{GeV}$), with at least two jets and $N_{\mathrm{b\,jets}} = 0$, $p_{\mathrm{T}}^{\mathrm{miss}} > 80\,\mathrm{GeV}$, and $M_{\mathrm{T2}}(\ell\ell) > 100\,\mathrm{GeV}$. The hatched band shows the uncertainties from experimental effects, as described in Section 7.

7 Systematic uncertainties and signal acceptance

Several experimental uncertainties affect the various signal and background yield estimations. Efficiencies of the dilepton triggers, as mentioned previously, range from 95 to 99%. The uncertainties in these efficiencies are about 1%. Offline lepton reconstruction and selection efficiencies are measured using $\mathrm{Z} \to \ell\ell$ events in bins of lepton p_{T} and pseudorapidity, and as a function of the total hadronic activity in the vicinity of the lepton. These measurements are performed separately in data and in simulation. Typical efficiency values range from 70 to 80%, and scale factors are used to correct the differences between data and simulation. The uncertainties in these scale factors are less than 3% per lepton in most of the search and control regions.

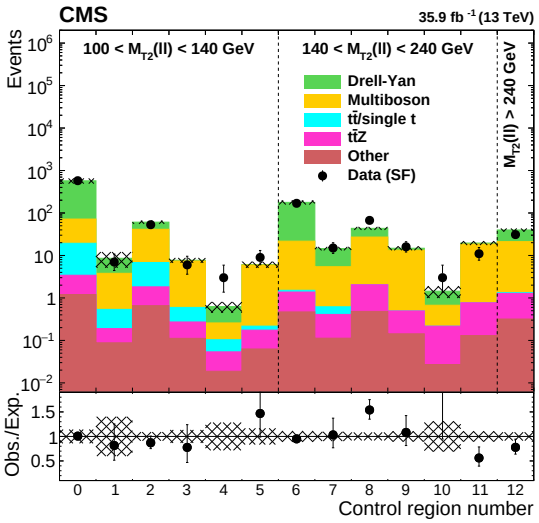

Figure 6: Event yields in the 13 Drell–Yan and multiboson control regions for events with SF leptons falling within the Z boson mass window ($|m(\ell\ell) - m_{\mathrm{Z}}| < 15\,\mathrm{GeV}$) and $N_{\mathrm{b\,jets}} = 0$, after renormalizing with the scale factors obtained from the fit procedure described in the text. The hatched band shows the uncertainties from the fit including the uncertainties from the experimental effects, as described in Section 7.

Uncertainties in the event yields resulting from the calibration of the jet energy scale are estimated by shifting the jet momenta in the simulation up and down by one standard deviation of the jet energy corrections. Depending on the jet p_{T} and η, the resulting uncertainty in the simulated yields from the jet energy scale is typically 1–5%, except in the lowest regions in $M_{\mathrm{T2}}(\ell\ell)$ where it can be as high as 12%. In addition, the energy scale of deposits from soft particles that are not clustered in jets are varied within their uncertainties and the resulting uncertainty reaches 3.5%, with an increase up to 25% in the lowest $M_{\mathrm{T2}}(\ell\ell)$ region. The b tagging efficiency in the simulation is corrected using scale factors determined from data [69], and uncertainties are propagated to all simulated events. These contribute an uncertainty of about 1–6% in the predicted yields depending on the transverse momentum and pseudorapidity of the b-tagged jet.

The effect of all the experimental uncertainties described above is evaluated for each of the simulated processes in all signal regions, and is considered correlated across the analysis bins and simulated processes.

Further experimental uncertainties arise from the normalization of the single top and top quark pair, Drell–Yan, and multiboson backgrounds in their respective control regions, for which uncertainties in the scale factors derived in Section 6 are taken into account. Finally, the uncertainty in the integrated luminosity is 2.5% [72].

Several additional systematic uncertainties affect the modeling in simulation of the various processes. Firstly, all simulated samples are reweighted according to the distribution of the true number of interactions at each bunch crossing. The uncertainty in the total inelastic pp cross section leads to uncertainties of 1–6% in the expected yields.

For the $\mathrm{t\bar{t}}$ and $\mathrm{t\bar{t}Z}$ backgrounds, we determine the event yield changes resulting from varying the renormalization and factorization scales by a factor of two, while keeping the overall normalization from the control region in data constant. We assign as uncertainty the envelope of the considered yield variations, treated uncorrelated between the background processes. Uncertainties in the PDFs can have a further effect on the simulated $M_{\mathrm{T2}}(\ell\ell)$ shape. We determine

the change of acceptance in the signal regions using the PDF variations and assign the envelope of these variations—between 1 and 6%—as a correlated uncertainty [73].

Measurements of the top quark p_T in $t\bar{t}$ events at $\sqrt{s} = 8$ and 13 TeV show a potential mismodeling in simulation [74, 75]. To evaluate the impact of this effect, we reweight the top quark p_T in the simulated $t\bar{t}$ sample to match that in data, keeping the overall normalization constant. The difference relative to the unweighted $t\bar{t}$ sample is assigned as a systematic uncertainty, which typically contributes an uncertainty of about 1–2% in the predicted yields.

For the small contribution from top quark pair production in association with a W or a Higgs boson, we take an uncertainty of 20% in the cross section based on the variations of the renormalization and factorization scales and the PDFs.

Finally, the statistical uncertainties due to the finite number of simulated events are treated as fully uncorrelated. These maximally amount to 27% on the rare backgrounds, with little impact on the analysis sensitivity.

A summary of the systematic uncertainties in the background prediction is presented in Table 3.

Most of the sources of systematic uncertainties in the background estimates affect the prediction of the signal as well, and these are evaluated separately for each mass configuration of the considered simplified models. We further estimate the effect of missing higher-order corrections for the signal acceptance by varying the renormalization and factorization scales [76, 77] and find that uncertainties are between 1 and 19%. The modeling of initial-state radiation (ISR) is relevant for the SUSY signal simulation in cases where the mass difference between the top squark and the LSP is small. The ISR reweighting is obtained in an inclusive data control region requiring an opposite-charge electron-muon pair and exactly two b jets, and is based on the number of ISR jets (N_J^{ISR}) not tagged as b jets, so as to make the jet multiplicity agree with data. The reweighting procedure is applied to SUSY Monte Carlo events and factors vary between 0.92 and 0.51 for N_J^{ISR} between 1 and 6. We take one half of the deviation from unity as the systematic uncertainty in these reweighting factors, correlated across search regions. It is generally found to have a small effect, but can reach 30% for compressed mass configurations. An uncertainty from potential differences of the modeling of p_T^{miss} in the fast simulation of the CMS detector with respect to data is evaluated by comparing the reconstructed p_T^{miss} with the p_T^{miss} obtained using generator-level information. This uncertainty ranges up to 20% and only affects the considered SUSY signal samples. For these samples, the scale factors and uncertainties for the tagging efficiency of b jets and leptons as well as the uncertainty on the modeling of pileup are evaluated separately. For DM signal models, the uncertainty in the signal acceptance due to variations of the PDFs is considered, while for the SUSY signal models, this uncertainty was found to be redundant with the ISR uncertainty and thus not included.

8 Results

No significant deviation from the SM prediction is observed in any of the signal regions. Good agreement between the predicted and observed $M_{T2}(\ell\ell)$, $M_{T2}(b\ell b\ell)$, and p_T^{miss} distributions is observed, as shown in Figs. 7 and 8, respectively. A summary of the predicted and observed event yields for each signal region is shown in Figs. 9 and 10 and in Table 4.

We interpret the results in the context of simplified SUSY models and combine with complementary results from the searches in the all-hadronic [20] and the single-lepton [19] final states for the T2tt and T2bW models. Moreover, we also interpret the results in a model with DM particle pair production via a scalar or pseudoscalar mediator.

Table 3: Relative systematic uncertainties in the background yields in the signal regions. Where given, ranges represent the minimal and maximal changes in yield across all signal regions.

Source of systematic uncertainty	Change in signal region yields (%)
Trigger efficiency	1
Lepton scale factors	1–5
Jet energy scale	1–12
Modeling of unclustered energy	1–25
b tagging	1–6
Top quark background normalization	3–20
$t\bar{t}Z$ background normalization	1–14
Multiboson background normalization	1–8
Drell-Yan background normalization	1–7
Integrated luminosity	2.5
Pileup modeling	1–6
Factorization/renormalization scales	1–19
PDFs	1–6
Top quark p_{T} modeling	1–2
$t\bar{t}X$ (excl. $t\bar{t}Z$) background normalization	1–6
Simulated sample event count	2–27

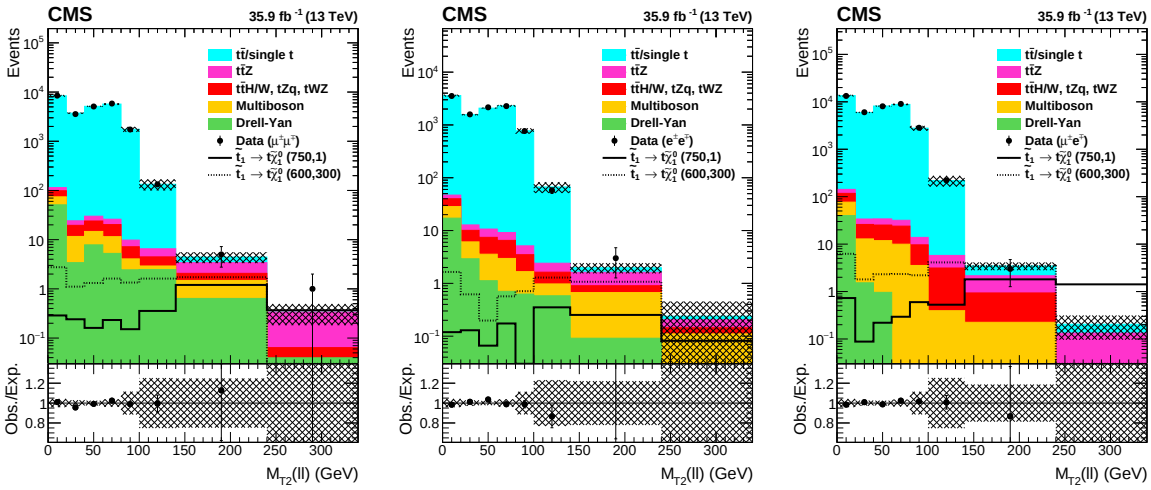

Figure 7: Distributions of $M_{\mathrm{T2}}(\ell\ell)$ for observed events in the $\mu\mu$ (left), ee (middle), and eμ (right) channels compared to the predicted SM backgrounds for the selection defined in Table 1. The hatched band shows the uncertainties discussed in the text.

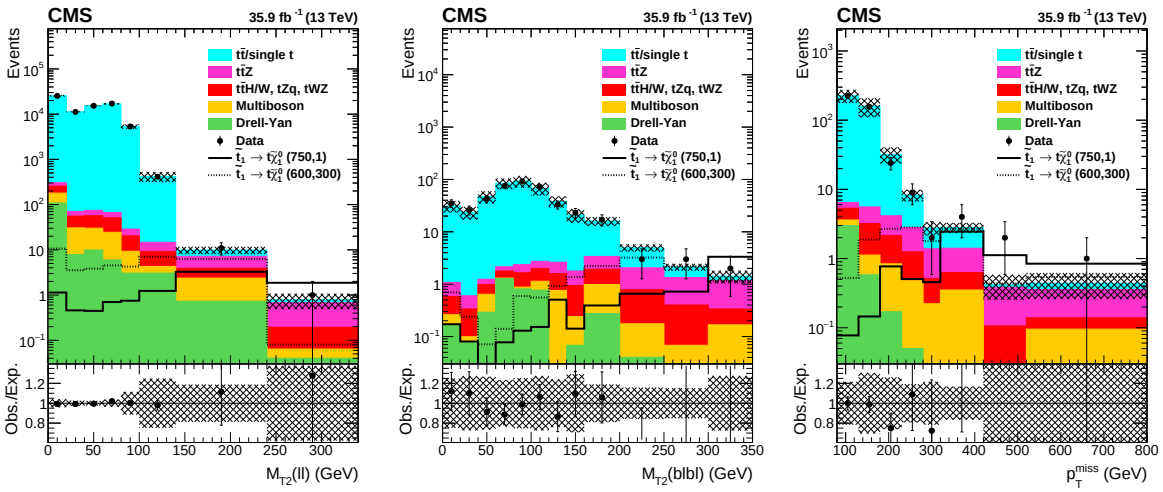

Figure 8: Distributions of $M_{\mathrm{T2}}(\ell\ell)$ (left), $M_{\mathrm{T2}}(\mathrm{b}\ell\mathrm{b}\ell)$ (middle), and $p_{\mathrm{T}}^{\mathrm{miss}}$ (right) for all lepton flavors for the selection defined in Table 1. Additionally, $M_{\mathrm{T2}}(\ell\ell) > 100\,\mathrm{GeV}$ is required for the $M_{\mathrm{T2}}(\mathrm{b}\ell\mathrm{b}\ell)$ and $p_{\mathrm{T}}^{\mathrm{miss}}$ distributions. The hatched band shows the uncertainties discussed in the text.

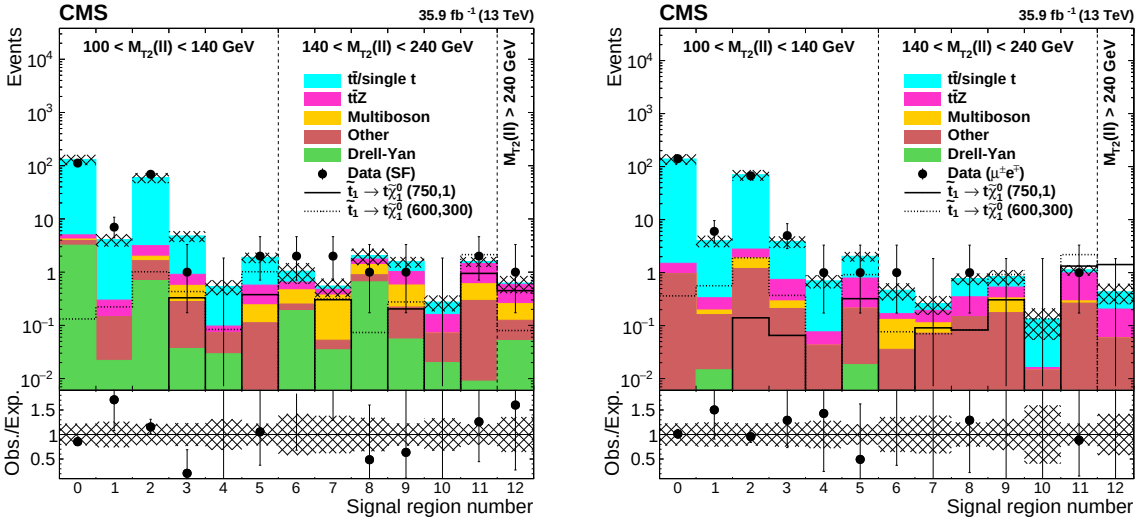

Figure 9: Predicted backgrounds and observed yields in the ee and $\mu\mu$ search regions (left) and the eμ search regions (right). The hatched band shows the uncertainties discussed in the text.

To perform the statistical interpretations, a likelihood function is formed containing Poisson probability functions for all data regions, where the same-flavor and different-flavor signal regions are considered separately. The control regions for the tt̄Z background and for the Drell–Yan and multiboson backgrounds, as depicted in Figs. 4 and 6, respectively, are included as well. The correlations of the uncertainties are taken into account as described in Section 7. A profile likelihood ratio in the asymptotic approximation [78] is used as the test statistic. Upper limits on the production cross section are then calculated at 95% confidence level (CL) using the asymptotic $\mathrm{CL_s}$ criterion [79, 80].

The SUSY interpretations are given in the $m_{\tilde{t}_1}$–$m_{\tilde{\chi}^0_1}$ plane in Figs. 11 and 12. The color on the z axis indicates the 95% CL upper limit on the cross section times the square of the branching fraction at each point in the $m_{\tilde{t}_1}$–$m_{\tilde{\chi}^0_1}$ plane. The area below the thick black curve represents the observed exclusion region at 95% CL assuming 100% branching fraction, while the dashed red

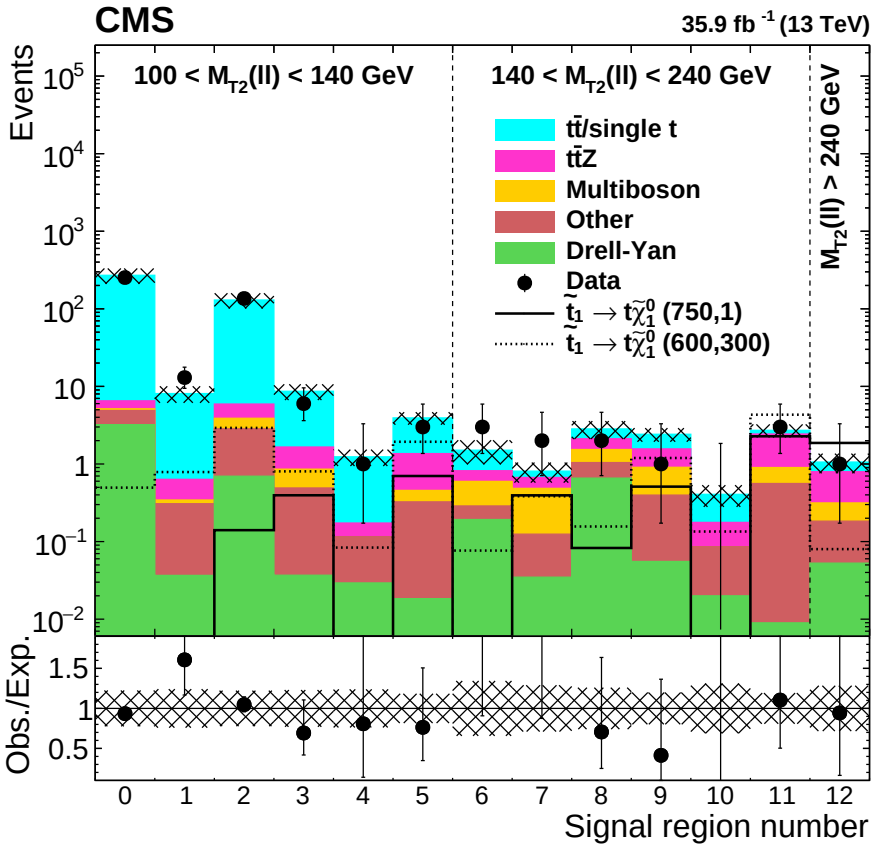

Figure 10: Predicted backgrounds and observed yields in the ee, $\mu\mu$, and eμ search regions combined. The hatched band shows the uncertainties discussed in the text.

lines indicate the expected limit at 95% CL and the region containing 68% of the distribution of limits expected under the background-only hypothesis. The thin black lines show the effect of the theoretical uncertainties in the signal cross section. In the T2tt model we exclude mass configurations with $m_{\tilde{\chi}_1^0}$ up to 360 GeV and $m_{\tilde{t}_1}$ up to 800 GeV, assuming that the top quarks are unpolarized. Because this choice may have a significant impact on the kinematic properties of the final state particles [81], we also check that for purely right-handed polarization, the limit increases by about 50 GeV in both $m_{\tilde{t}_1}$ and $m_{\tilde{\chi}_1^0}$, while for purely left-handed polarization, the limit decreases by about 50 GeV in $m_{\tilde{t}_1}$ and by 70 GeV in $m_{\tilde{\chi}_1^0}$.

The results for the T2bW and T8bb$\ell\ell\nu\nu$ models are shown in Figs. 11 (right) and 12. We exclude mass configurations with $m_{\tilde{\chi}_1^0}$ up to 320 GeV and $m_{\tilde{t}_1}$ up to 750 GeV in the T2bW model. The sensitivity in the T8bb$\ell\ell\nu\nu$ model strongly depends on the intermediate slepton mass and is largest when $x = 0.95$ in $m_{\tilde{\ell}} = x\,(m_{\tilde{\chi}_1^+} - m_{\tilde{\chi}_1^0}) + m_{\tilde{\chi}_1^0}$. In this case, excluded masses reach up to 800 GeV for $m_{\tilde{\chi}_1^0}$ and 1300 GeV for $m_{\tilde{t}_1}$. These numbers reduce to 660 GeV for $m_{\tilde{\chi}_1^0}$ and 1200 GeV for $m_{\tilde{t}_1}$ when $x = 0.5$ and to 50 GeV for $m_{\tilde{\chi}_1^0}$ and 1000 GeV for $m_{\tilde{t}_1}$ when $x = 0.05$.

Besides the dilepton search described in this paper, searches for direct top squark pair production were also performed in final states with a single lepton [19] and without leptons [20]. The signal and control regions for these two searches and the dilepton search are mutually exclusive. A statistical combination of the results of the three searches is performed in the context of the T2tt and T2bW scenarios of top squark pair production, taking into account correlations in both signal and expected background yields in the different analyses. Figure 13 shows the combination of the results of the three searches for direct top squark pair production for the

Table 4: Total expected background and event yields in data in each of the signal regions for same-flavor ($e^+e^-/\mu^+\mu^-$), different-flavor ($e^\pm\mu^\mp$), and all channels combined with all the systematic uncertainties included as described in Section 7.

Signal region	Same flavor		Different flavor		All	
	Expected	Observed	Expected	Observed	Expected	Observed
0	131 ± 30	112	139 ± 32	141	271 ± 61	253
1	4.1 ± 1.1	7	4.0 ± 1.1	6	8.1 ± 2.0	13
2	60 ± 13	69	70 ± 17	67	130 ± 29	136
3	4.8 ± 1.2	1	3.9 ± 1.0	5	8.7 ± 2.0	6
4	0.5 ± 0.2	0	0.7 ± 0.2	1	1.2 ± 0.4	1
5	1.9 ± 0.5	2	2.1 ± 0.5	1	4.0 ± 0.8	3
6	1.1 ± 0.6	2	0.5 ± 0.2	1	1.5 ± 0.7	3
7	0.6 ± 0.3	2	0.3 ± 0.2	0	0.8 ± 0.3	2
8	2.1 ± 0.7	1	0.8 ± 0.2	1	2.9 ± 0.7	2
9	1.6 ± 0.4	1	0.9 ± 0.3	0	2.5 ± 0.5	1
10	0.3 ± 0.1	0	0.1 ± 0.1	0	0.4 ± 0.2	0
11	1.7 ± 0.4	2	1.2 ± 0.3	1	2.9 ± 0.6	3
12	0.7 ± 0.3	1	0.5 ± 0.2	0	1.1 ± 0.4	1

T2tt model with $\widetilde{t}_1 \to t\widetilde{\chi}_1^0$ decays. The combined result excludes a top squark mass of 1050 GeV for a massless LSP, and an LSP mass of 500 GeV for a top squark mass of 900 GeV. The combination is driven primarily by the all-jet search, except in the region of small mass splitting between the top squark and the LSP where searches in the zero- and one-lepton channels have similar sensitivity. Figure 14 shows the equivalent limits for direct top squark pair production for the T2bW model with $\widetilde{t}_1 \to b\widetilde{\chi}_1^+, \widetilde{\chi}_1^+ \to W^+\widetilde{\chi}_1^0$ decays. The combined result for this scenario excludes a top squark mass of 1000 GeV for a massless LSP and an LSP mass of 450 GeV for a top squark mass of 900 GeV. The combination extends the sensitivity to both top squark and LSP masses by about 50 GeV compared to the most sensitive individual result coming from the one-lepton channel.

Limits on the production of DM particle pairs in association with top quark pairs via a scalar or pseudoscalar mediator are listed in Table 5, assuming $g_q = g_{DM} = 1$. The results are presented as ratios $\mu = \sigma/\sigma_{theory}$ of the 95% CL expected and observed upper limits on the cross section σ with respect to the simplified model cross section expectations σ_{theory}. Results are shown for different DM particle and mediator masses, and for both scalar and pseudoscalar mediators. Figure 15 shows expected and observed limits as a function of the mediator mass for DM particles χ with a mass of 1 GeV. We exclude scalar mediators with masses up to 100 GeV and pseudoscalar mediators with masses up to 50 GeV.

In order to facilitate the reinterpretation of these results, we construct three aggregate signal regions. The preselection in Table 1 is applied, but in contrast to the main analysis, there is no separation of events according to lepton flavor. Regions A0 and A1 are defined as $100 \leq M_{T2}(\ell\ell) < 140$ GeV and $140 \leq M_{T2}(\ell\ell) < 240$ GeV, with an additional requirement of $p_T^{miss} > 200$ GeV for both. Region A2 is defined by $M_{T2}(\ell\ell) > 240$ GeV and $p_T^{miss} > 80$ GeV. Expected and observed yields in the aggregate regions are shown in Table 6. The covariance and correlation matrices [82] for the background predictions in the aggregate regions are given in Table 7.

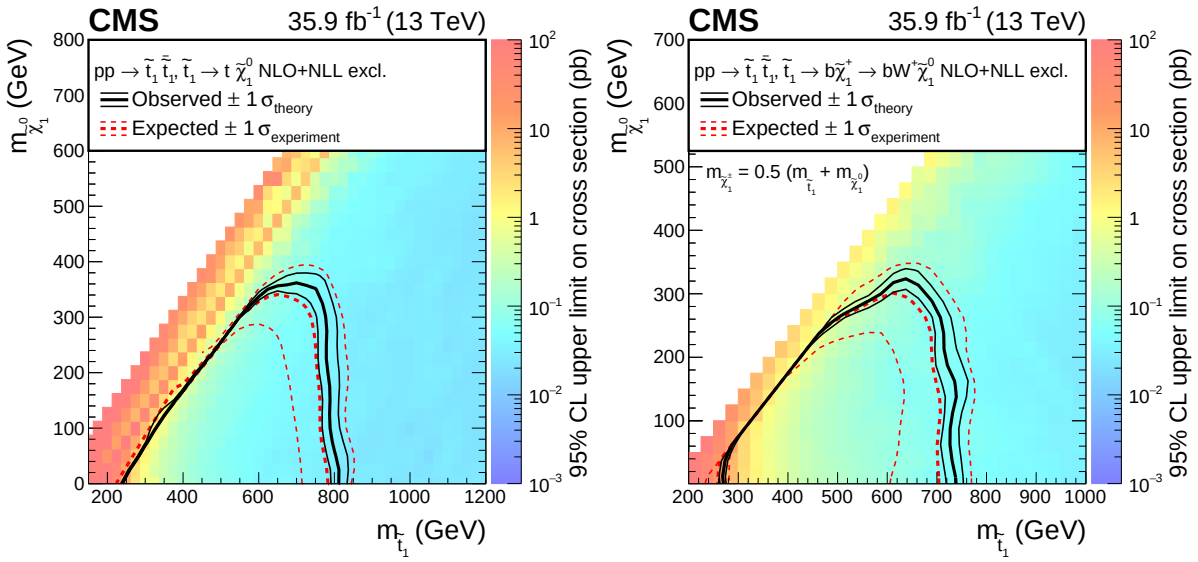

Figure 11: Expected and observed limits for the T2tt model with $\tilde{t}_1 \to t\tilde{\chi}^0_1$ decays (left) and for the T2bW model with $\tilde{t}_1 \to b\tilde{\chi}^+_1 \to bW^+\tilde{\chi}^0_1$ decays (right) in the $m_{\tilde{t}_1}$–$m_{\tilde{\chi}^0_1}$ mass plane. The color indicates the 95% CL upper limit on the cross section times the square of the branching fraction at each point in the plane. The area below the thick black curve represents the observed exclusion region at 95% CL assuming 100% branching fraction, while the dashed red lines indicate the expected limits at 95% CL and the region containing 68% of the distribution of limits expected under the background-only hypothesis. The thin black lines show the effect of the theoretical uncertainties in the signal cross section.

9 Summary

A search was presented for top squark pair production and dark matter in final states with two leptons, b jets, and large missing transverse momentum in data corresponding to an integrated luminosity of 35.9 fb^{-1} in pp collisions collected at a center-of-mass energy of 13 TeV in the CMS detector at the LHC. An efficient background reduction using dedicated kinematic variables was achieved, suppressing by several orders of magnitude the large background from standard model dilepton $\text{t}\bar{\text{t}}$ events. With no evidence observed for a deviation from the expected background from the standard model, results were interpreted in several simplified models for supersymmetric top squark pair production as well as through the production of a spin-0 dark matter mediator in association with a $\text{t}\bar{\text{t}}$ pair.

In the T2tt model with $\tilde{t}_1 \to t\tilde{\chi}^0_1$ decays, $\tilde{t}_1$ masses <800 GeV and $\tilde{\chi}^0_1$ masses <360 GeV are excluded. In the T2bW model with $\tilde{t}_1 \to b\tilde{\chi}^+_1 \to bW^+\tilde{\chi}^0_1$ decays, $\tilde{t}_1$ masses <750 GeV and $\tilde{\chi}^0_1$ masses <320 GeV are excluded, assuming the chargino mass to be the mean of the $\tilde{t}_1$ and the $\tilde{\chi}^0_1$ masses. In the newly considered T8bb$\ell\ell\nu\nu$ model with decays $\tilde{t}_1 \to b\tilde{\chi}^+_1 \to b\nu\tilde{\ell} \to b\nu\ell\tilde{\chi}^0_1$, and therefore 100% branching to dilepton final states, the sensitivity depends on the intermediate particle masses. With the chargino mass again taken as the mean of the $\tilde{t}_1$ and the $\tilde{\chi}^0_1$ masses, the strongest exclusion is obtained if the slepton mass is close to the chargino mass. In this case, excluded masses reach up to 1.3 TeV for $\tilde{t}_1$ and 800 GeV for $\tilde{\chi}^0_1$.

The T2tt and T2bW results were combined with complementary searches in the all-jet and single-lepton channels, providing exclusions in the T2tt model of $\tilde{t}_1$ mass <1050 GeV for a massless $\tilde{\chi}^0_1$, and a $\tilde{\chi}^0_1$ mass of <500 GeV for a $\tilde{t}_1$ mass of 900 GeV. In the same way, the T2bW model is excluded for $\tilde{t}_1$ mass <1000 GeV for a massless $\tilde{\chi}^0_1$, and a $\tilde{\chi}^0_1$ mass of <450 GeV for a $\tilde{t}_1$ mass of 900 GeV

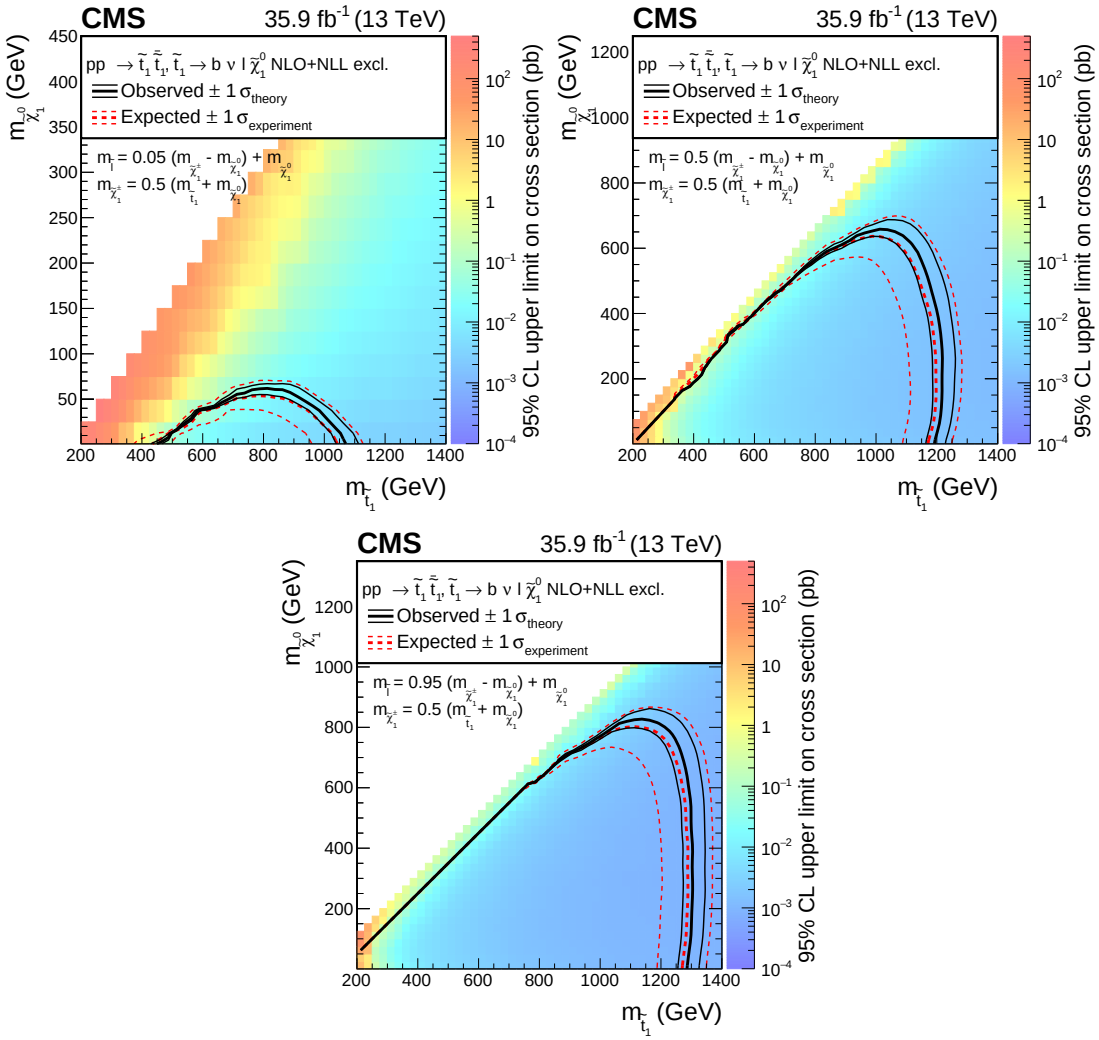

Figure 12: Expected and observed limits for the T8bb$\ell\ell\nu\nu$ model with $\tilde{t}_1 \to b\tilde{\chi}_1^+ \to b\nu\tilde{\ell} \to b\nu\ell\tilde{\chi}_1^0$ decays in the $m_{\tilde{t}_1}$–$m_{\tilde{\chi}_1^0}$ mass plane for three different mass configurations defined by $m_{\tilde{\ell}} = x\,(m_{\tilde{\chi}_1^+} - m_{\tilde{\chi}_1^0}) + m_{\tilde{\chi}_1^0}$ with $x = 0.05$ (upper left), $x = 0.5$ (upper right), and $x = 0.95$ (lower). The description of curves is the same as in the caption of Fig. 11.

The combination extends the sensitivity by ≈50 GeV in the masses of both $\tilde{t}_1$ and $\tilde{\chi}_1^0$ in the T2bW model, and by similar values in the T2tt model, when the difference between these masses is ≈200 GeV. Aggregate search regions were presented that can be used to reinterpret the results in a wider range of theoretical models of new physics that give rise to the chosen final state.

In addition, the results were interpreted in a simplified model with a dark matter candidate particle coupled to the top quark via a scalar or a pseudoscalar mediator. Within the assumptions of the model, a scalar mediator with a mass up to 100 GeV and a pseudoscalar mediator with a mass up to 50 GeV are excluded for a dark matter candidate mass of 1 GeV. The result for the scalar mediator achieves some of the most stringent limits to date in this model.

Acknowledgments

We congratulate our colleagues in the CERN accelerator departments for the excellent performance of the LHC and thank the technical and administrative staffs at CERN and at other

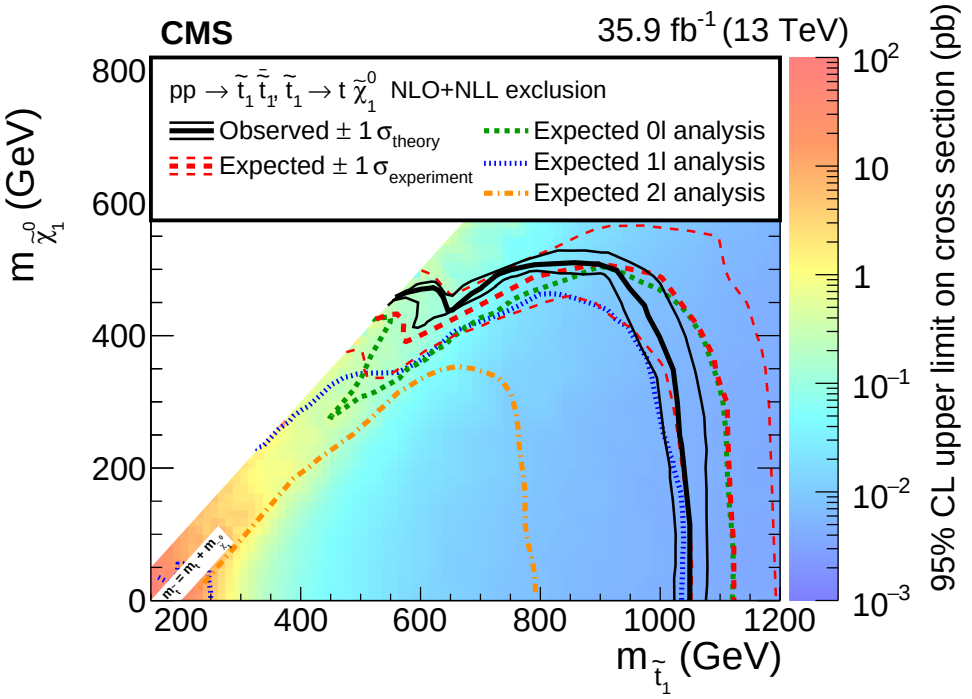

Figure 13: Expected and observed limits for the T2tt model with $\tilde{t}_1 \rightarrow t\tilde{\chi}_1^0$ decays in the $m_{\tilde{t}_1}$–$m_{\tilde{\chi}_1^0}$ mass plane combining the dilepton final state with the single-lepton [19] and the all-hadronic [20] final states as described in the text. The color indicates the 95% CL upper limit on the cross section times the square of the branching fraction at each point in the plane. The area below the thick black curve represents the observed exclusion region at 95% CL assuming 100% branching fraction, while the dashed red lines indicate the expected limits at 95% CL and the region containing 68% of the distribution of limits expected under the background-only hypothesis. The thin black lines show the effect of the theoretical uncertainties in the signal cross section. The green short-dashed, blue dotted, and long-short-dashed orange curves show the expected individual limits for the all-hadronic, single-lepton, and dilepton analyses, respectively. The whited out area on the diagonal corresponds to configurations where the mass difference between $\tilde{t}_1$ and $\tilde{\chi}_1^0$ is very close to the top quark mass. In this region the signal acceptance strongly depends on the $\tilde{\chi}_1^0$ mass and is therefore hard to model.

CMS institutes for their contributions to the success of the CMS effort. In addition, we gratefully acknowledge the computing centers and personnel of the Worldwide LHC Computing Grid for delivering so effectively the computing infrastructure essential to our analyses. Finally, we acknowledge the enduring support for the construction and operation of the LHC and the CMS detector provided by the following funding agencies: BMWFW and FWF (Austria); FNRS and FWO (Belgium); CNPq, CAPES, FAPERJ, and FAPESP (Brazil); MES (Bulgaria); CERN; CAS, MoST, and NSFC (China); COLCIENCIAS (Colombia); MSES and CSF (Croatia); RPF (Cyprus); SENESCYT (Ecuador); MoER, ERC IUT, and ERDF (Estonia); Academy of Finland, MEC, and HIP (Finland); CEA and CNRS/IN2P3 (France); BMBF, DFG, and HGF (Germany); GSRT (Greece); OTKA and NIH (Hungary); DAE and DST (India); IPM (Iran); SFI (Ireland); INFN (Italy); MSIP and NRF (Republic of Korea); LAS (Lithuania); MOE and UM (Malaysia); BUAP, CINVESTAV, CONACYT, LNS, SEP, and UASLP-FAI (Mexico); MBIE (New Zealand); PAEC (Pakistan); MSHE and NSC (Poland); FCT (Portugal); JINR (Dubna); MON, RosAtom, RAS, RFBR and RAEP (Russia); MESTD (Serbia); SEIDI, CPAN, PCTI and FEDER (Spain); Swiss Funding Agencies (Switzerland); MST (Taipei); ThEPCenter, IPST, STAR, and NSTDA (Thailand); TUBITAK and TAEK (Turkey); NASU and SFFR (Ukraine); STFC (United

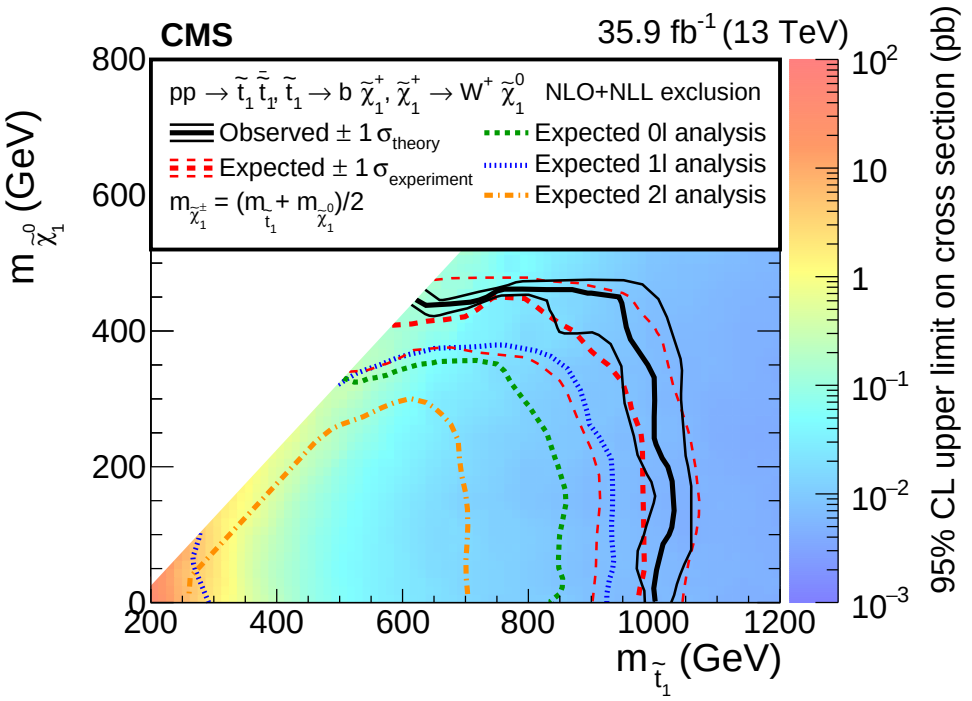

Figure 14: Expected and observed limits for the T2bW model with $\tilde{t}_1 \to b\tilde{\chi}_1^+ \to bW^+\tilde{\chi}_1^0$ decays in the $m_{\tilde{t}_1}$–$m_{\tilde{\chi}_1^0}$ mass plane combining the dilepton final state with the all-hadronic [20] and the single-lepton [19] final states as described in the text. The mass of the chargino is chosen to be $(m_{\tilde{t}_1} + m_{\tilde{\chi}_1^0})/2$. The description of curves is the same as in the caption of Fig. 13.

Kingdom); DOE and NSF (USA).

Individuals have received support from the Marie-Curie program and the European Research Council and Horizon 2020 Grant, contract No. 675440 (European Union); the Leventis Foundation; the A. P. Sloan Foundation; the Alexander von Humboldt Foundation; the Belgian Federal Science Policy Office; the Fonds pour la Formation à la Recherche dans l'Industrie et dans l'Agriculture (FRIA-Belgium); the Agentschap voor Innovatie door Wetenschap en Technologie (IWT-Belgium); the Ministry of Education, Youth and Sports (MEYS) of the Czech Republic; the Council of Science and Industrial Research, India; the HOMING PLUS program of the Foundation for Polish Science, cofinanced from European Union, Regional Development Fund, the Mobility Plus program of the Ministry of Science and Higher Education, the National Science Center (Poland), contracts Harmonia 2014/14/M/ST2/00428, Opus 2014/13/B/ST2/02543, 2014/15/B/ST2/03998, and 2015/19/B/ST2/02861, Sonata-bis 2012/07/E/ST2/01406; the National Priorities Research Program by Qatar National Research Fund; the Programa Severo Ochoa del Principado de Asturias; the Thalis and Aristeia programs cofinanced by EU-ESF and the Greek NSRF; the Rachadapisek Sompot Fund for Postdoctoral Fellowship, Chulalongkorn University and the Chulalongkorn Academic into Its 2nd Century Project Advancement Project (Thailand); the Welch Foundation, contract C-1845; and the Weston Havens Foundation (USA).

References

[1] E. Witten, "Dynamical breaking of supersymmetry", *Nucl. Phys. B* **188** (1981) 513, doi:10.1016/0550-3213(81)90006-7.

[2] S. Dimopoulos and H. Georgi, "Softly broken supersymmetry and SU(5)", *Nucl. Phys. B*

Table 5: Ratios $\mu = \sigma/\sigma_{\text{theory}}$ of the 95% CL expected and observed limits to simplified model expectations for different DM particle masses and mediator masses and for scalar (ϕ) and pseudoscalar (a) mediators under the assumption $g_{\text{q}} = g_{\text{DM}} = 1$. The uncertainties reflect the 68% band of the expected limits.

m_χ	$m_{\phi/\text{a}}$	Scalar			Pseudoscalar		
(GeV)	(GeV)	σ_{theory} (fb)	Expected	Observed	σ_{theory} (fb)	Expected	Observed
1	10	21357	$0.54^{+0.25}_{-0.16}$	0.70	451	$1.01^{+0.49}_{-0.32}$	0.81
1	20	10954	$0.56^{+0.26}_{-0.17}$	0.53	411	$1.02^{+0.49}_{-0.32}$	0.81
1	50	3086	$0.67^{+0.32}_{-0.21}$	0.59	308	$1.14^{+0.55}_{-0.36}$	0.91
1	100	720	$1.04^{+0.48}_{-0.32}$	0.90	193	$1.33^{+0.65}_{-0.42}$	1.08
1	200	101	$2.30^{+1.11}_{-0.72}$	1.87	87.8	$2.02^{+1.01}_{-0.64}$	1.64
1	300	30.5	$4.8^{+2.3}_{-1.5}$	3.8	39.5	$3.7^{+1.8}_{-1.2}$	2.9
1	500	4.95	$21.6^{+10.9}_{-6.9}$	17.4	5.14	$21.0^{+10.4}_{-6.7}$	16.9
10	10	101	$18.8^{+8.8}_{-5.8}$	16.6	15.2	$19.3^{+9.3}_{-6.1}$	15.3
10	15	127	$17.0^{+8.0}_{-5.2}$	13.8	19.5	$15.8^{+7.6}_{-5.0}$	12.7
10	50	3096	$0.72^{+0.33}_{-0.22}$	0.69	310	$1.08^{+0.52}_{-0.34}$	0.86
10	100	742	$1.03^{+0.48}_{-0.32}$	0.84	197	$1.25^{+0.61}_{-0.39}$	0.98
50	10	2.10	125^{+61}_{-39}	102	2.38	72^{+36}_{-23}	58
50	50	2.57	104^{+50}_{-33}	84	2.95	62^{+30}_{-19}	49
50	95	7.24	52^{+25}_{-16}	43	10.8	$20.3^{+10.0}_{-6.4}$	16.2
50	200	100	$2.32^{+1.14}_{-0.73}$	1.86	84.8	$2.05^{+1.02}_{-0.64}$	1.64
50	300	30.5	$4.7^{+2.3}_{-1.5}$	3.8	38.5	$3.7^{+1.9}_{-1.2}$	3.0

Table 6: Expected and observed event yields, summed over all lepton flavors, in the aggregate signal regions defined by the selection requirements in the table.

Signal region	$p_{\text{T}}^{\text{miss}}$ (GeV)	$M_{\text{T2}}(\ell\ell)$ (GeV)	Expected	Observed
A0	>200	100–140	20.8 ± 4.4	22
A1	>200	140–240	6.2 ± 1.0	6
A2	>80	>240	1.1 ± 0.4	1

193 (1981) 150, doi:10.1016/0550-3213(81)90522-8.

[3] P. Ramond, "Dual theory for free fermions", *Phys. Rev. D* **3** (1971) 2415, doi:10.1103/PhysRevD.3.2415.

[4] Y. A. Gol'fand and E. P. Likhtman, "Extension of the algebra of Poincaré group generators and violation of P invariance", *JETP Lett.* **13** (1971) 323.

[5] A. Neveu and J. H. Schwarz, "Factorizable dual model of pions", *Nucl. Phys. B* **31** (1971) 86, doi:10.1016/0550-3213(71)90448-2.

[6] D. V. Volkov and V. P. Akulov, "Possible universal neutrino interaction", *JETP Lett.* **16** (1972) 438.

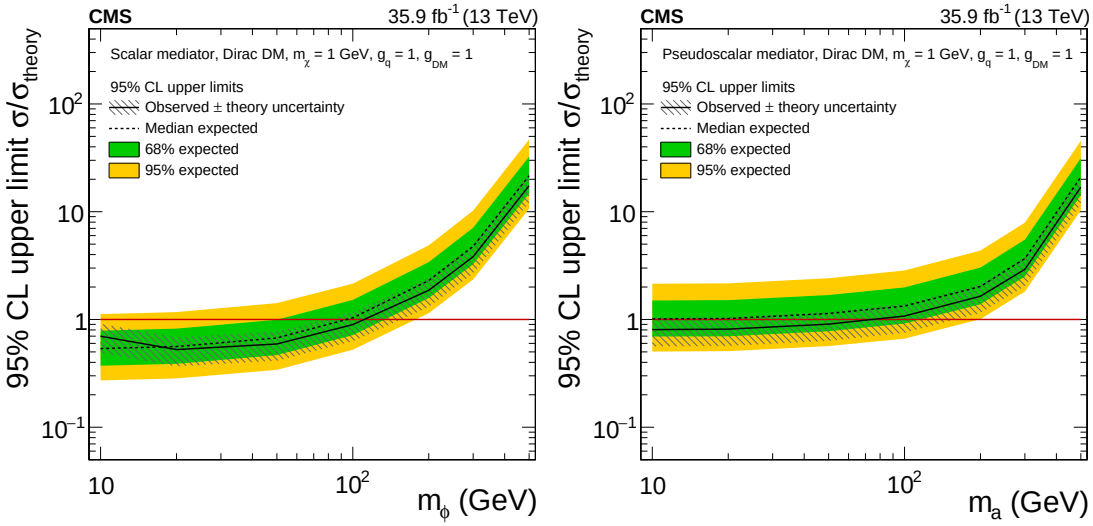

Figure 15: The 95% CL expected (dashed line) and observed limits (solid line) on $\mu = \sigma/\sigma_{\text{theory}}$ for a fermionic DM particle with $m_\chi = 1\,\text{GeV}$ assuming different scalar (left) and pseudoscalar (right) mediator masses. The green and yellow bands represent the regions containing 68 and 95%, respectively, of the distribution of limits expected under the background-only hypothesis. The horizontal red line indicates $\mu = 1$. The mediator couplings are set to $g_\text{q} = g_\text{DM} = 1$. The gray hashed band around the observed limit corresponds to a 30% theory uncertainty in the inclusive signal cross section.

Table 7: Covariance (left) and correlation matrix (right) for the background prediction in the aggregate signal regions described in Table 6.

Covariance			
	A0	A1	A2
A0	13.3	1.8	0.5
A1		0.9	0.2
A2			0.1

Correlation			
	A0	A1	A2
A0	1	0.51	0.38
A1		1	0.49
A2			1

[7] J. Wess and B. Zumino, "A lagrangian model invariant under supergauge transformations", *Phys. Lett. B* **49** (1974) 52, doi:10.1016/0370-2693(74)90578-4.

[8] J. Wess and B. Zumino, "Supergauge transformations in four dimensions", *Nucl. Phys. B* **70** (1974) 39, doi:10.1016/0550-3213(74)90355-1.

[9] P. Fayet, "Supergauge invariant extension of the Higgs mechanism and a model for the electron and its neutrino", *Nucl. Phys. B* **90** (1975) 104, doi:10.1016/0550-3213(75)90636-7.

[10] H. P. Nilles, "Supersymmetry, supergravity and particle physics", *Phys. Rep.* **110** (1984) 1, doi:10.1016/0370-1573(84)90008-5.

[11] G. R. Farrar and P. Fayet, "Phenomenology of the production, decay, and detection of new hadronic states associated with supersymmetry", *Phys. Lett. B* **76** (1978) 575, doi:10.1016/0370-2693(78)90858-4.

[12] M. Papucci, J. T. Ruderman, and A. Weiler, "Natural SUSY endures", *JHEP* **09** (2012) 035, doi:10.1007/JHEP09(2012)035, arXiv:1110.6926.

[13] J. Smith, W. L. van Neerven, and J. A. M. Vermaseren, "The transverse mass and width of the W boson", *Phys. Rev. Lett.* **50** (1983) 1738, doi:10.1103/PhysRevLett.50.1738.

[14] C. G. Lester and D. J. Summers, "Measuring masses of semiinvisibly decaying particles pair produced at hadron colliders", *Phys. Lett. B* **463** (1999) 99, doi:10.1016/S0370-2693(99)00945-4, arXiv:hep-ph/9906349.

[15] J. Alwall, P. Schuster, and N. Toro, "Simplified models for a first characterization of new physics at the LHC", *Phys. Rev. D* **79** (2009) 075020, doi:10.1103/PhysRevD.79.075020, arXiv:0810.3921.

[16] J. Alwall, M.-P. Le, M. Lisanti, and J. G. Wacker, "Model-independent jets plus missing energy searches", *Phys. Rev. D* **79** (2009) 015005, doi:10.1103/PhysRevD.79.015005, arXiv:0809.3264.

[17] LHC New Physics Working Group Collaboration, "Simplified models for LHC new physics searches", *J. Phys. G* **39** (2012) 105005, doi:10.1088/0954-3899/39/10/105005, arXiv:1105.2838.

[18] CMS Collaboration, "Interpretation of searches for supersymmetry with simplified models", *Phys. Rev. D* **88** (2013) 052017, doi:10.1103/PhysRevD.88.052017, arXiv:1301.2175.

[19] CMS Collaboration, "Search for top squark pair production in pp collisions at $\sqrt{s}$ = 13 TeV using single lepton events", *JHEP* **10** (2017) 019, doi:10.1007/JHEP10(2017)019, arXiv:1706.04402.

[20] CMS Collaboration, "Search for direct production of supersymmetric partners of the top quark in the all-jets final state in proton-proton collisions at $\sqrt{s} = 13\,\text{TeV}$", *JHEP* **10** (2017) 005, doi:10.1007/JHEP10(2017)005, arXiv:1707.03316.

[21] CMS Collaboration, "Search for top-squark pair production in the single-lepton final state in pp collisions at $\sqrt{s} = 8\,\text{TeV}$", *Eur. Phys. J. C* **73** (2013) 2677, doi:10.1140/epjc/s10052-013-2677-2, arXiv:1308.1586.

[22] CMS Collaboration, "Search for direct pair production of scalar top quarks in the single- and dilepton channels in proton-proton collisions at $\sqrt{s} = 8$ TeV", *JHEP* **07** (2016) 027, doi:10.1007/JHEP07(2016)027, arXiv:1602.03169. [Erratum: doi:10.1007/JHEP09(2016)056].

[23] CMS Collaboration, "Searches for pair production of third-generation squarks in $\sqrt{s} = 13$ TeV pp collisions", *Eur. Phys. J. C* **77** (2017) 327, doi:10.1140/epjc/s10052-017-4853-2, arXiv:1612.03877.

[24] ATLAS Collaboration, "Search for direct top squark pair production in final states with two leptons in $\sqrt{s} = 13$ TeV pp collisions with the ATLAS detector", (2017). arXiv:1708.03247.

[25] ATLAS Collaboration, "ATLAS Run 1 searches for direct pair production of third-generation squarks at the Large Hadron Collider", *Eur. Phys. J. C* **75** (2015) 510, doi:10.1140/epjc/s10052-015-3726-9, arXiv:1506.08616. [Erratum: doi:10.1140/epjc/s10052-016-3935-x].

[26] ATLAS Collaboration, "Search for top squark pair production in final states with one isolated lepton, jets, and missing transverse momentum in $\sqrt{s} = 8$ TeV pp collisions with the ATLAS detector", *JHEP* **11** (2014) 118, doi:10.1007/JHEP11(2014)118, arXiv:1407.0583.

[27] ATLAS Collaboration, "Search for direct top-squark pair production in final states with two leptons in pp collisions at $\sqrt{s} = 8$ TeV with the ATLAS detector", *JHEP* **06** (2014) 124, doi:10.1007/JHEP06(2014)124, arXiv:1403.4853.

[28] ATLAS Collaboration, "Search for top squarks in final states with one isolated lepton, jets, and missing transverse momentum in $\sqrt{s} = 13$ TeV pp collisions with the ATLAS detector", *Phys. Rev. D* **94** (2016) 052009, doi:10.1103/PhysRevD.94.052009, arXiv:1606.03903.

[29] T. Lin, E. W. Kolb, and L.-T. Wang, "Probing dark matter couplings to top and bottom quarks at the LHC", *Phys. Rev. D* **88** (2013) 063510, doi:10.1103/PhysRevD.88.063510, arXiv:1303.6638.

[30] M. R. Buckley, D. Feld, and D. Goncalves, "Scalar Simplified Models for Dark Matter", *Phys. Rev. D* **91** (2015) 015017, doi:10.1103/PhysRevD.91.015017, arXiv:1410.6497.

[31] U. Haisch and E. Re, "Simplified dark matter top-quark interactions at the LHC", *JHEP* **06** (2015) 078, doi:10.1007/JHEP06(2015)078, arXiv:1503.00691.

[32] C. Arina et al., "A comprehensive approach to dark matter studies: exploration of simplified top-philic models", *JHEP* **11** (2016) 111, doi:10.1007/JHEP11(2016)111, arXiv:1605.09242.

[33] D. Abercrombie et al., "Dark matter benchmark models for early LHC Run-2 searches: Report of the ATLAS/CMS dark matter forum", (2015). arXiv:1507.00966.

[34] G. D'Ambrosio, G. F. Giudice, G. Isidori, and A. Strumia, "Minimal flavor violation: an effective field theory approach", *Nucl. Phys.* **645** (2002) 155, doi:10.1016/S0550-3213(02)00836-2, arXiv:hep-ph/0207036.

[35] G. Isidori and D. M. Straub, "Minimal flavour violation and beyond", *Eur. Phys. J. C* **72** (2012) 2103, doi:10.1140/epjc/s10052-012-2103-1, arXiv:1202.0464.

[36] ATLAS Collaboration, "Search for dark matter in events with heavy quarks and missing transverse momentum in pp collisions with the ATLAS detector", *Eur. Phys. J. C* **75** (2015) 92, doi:10.1140/epjc/s10052-015-3306-z, arXiv:1410.4031.

[37] CMS Collaboration, "Search for the production of dark matter in association with top-quark pairs in the single-lepton final state in proton-proton collisions at $\sqrt{s}$ = 8 TeV", *JHEP* **06** (2015) 121, doi:10.1007/JHEP06(2015)121, arXiv:1504.03198.

[38] CMS Collaboration, "Search for dark matter produced in association with heavy-flavor quark pairs in proton-proton collisions at $\sqrt{s} = 13$ TeV", *Eur. Phys. J. C* **77** (2017) 845, doi:10.1140/epjc/s10052-017-5317-4, arXiv:1706.02581.

[39] CMS Collaboration, "Search for dark matter produced with an energetic jet or a hadronically decaying W or Z boson at $\sqrt{s} = 13$ TeV", *JHEP* **07** (2017) 014, doi:10.1007/JHEP07(2017)014, arXiv:1703.01651.

[40] ATLAS Collaboration, "Search for dark matter produced in association with bottom or top quarks in $\sqrt{s}$ = 13 TeV pp collisions with the ATLAS detector", (2017). arXiv:1710.11412.

[41] CMS Collaboration, "The CMS experiment at the CERN LHC", *JINST* **3** (2008) S08004, doi:10.1088/1748-0221/3/08/S08004.

[42] S. Alioli et al., "NLO single-top production matched with shower in POWHEG: s- and t-channel contributions", *JHEP* **09** (2009) 111, doi:10.1088/1126-6708/2009/09/111, arXiv:0907.4076.

[43] S. Alioli et al., "A general framework for implementing NLO calculations in shower Monte Carlo programs: the POWHEG BOX", *JHEP* **06** (2010) 043, doi:10.1007/JHEP06(2010)043, arXiv:1002.2581.

[44] M. Czakon and A. Mitov, "Top++: a program for the calculation of the top-pair cross-section at hadron colliders", *Comput. Phys. Commun.* **185** (2014) 2930, doi:10.1016/j.cpc.2014.06.021, arXiv:1112.5675.

[45] M. Aliev et al., "HATHOR: HAdronic Top and Heavy quarks crOss section calculatoR", *Comput. Phys. Commun.* **182** (2011) 1034, doi:10.1016/j.cpc.2010.12.040, arXiv:1007.1327.

[46] M. Beneke, P. Falgari, S. Klein, and C. Schwinn, "Hadronic top-quark pair production with NNLL threshold resummation", *Nucl. Phys. B* **855** (2012) 695, doi:10.1016/j.nuclphysb.2011.10.021, arXiv:1109.1536.

[47] M. Czakon and A. Mitov, "NNLO corrections to top pair production at hadron colliders: the all-fermionic scattering channels", *JHEP* **12** (2012) 054, doi:10.1007/JHEP12(2012)054, arXiv:1207.0236.

[48] M. Czakon and A. Mitov, "NNLO corrections to top pair production at hadron colliders: the quark-gluon reaction", *JHEP* **01** (2013) 080, doi:10.1007/JHEP01(2013)080, arXiv:1210.6832.

[49] M. Czakon, P. Fiedler, and A. Mitov, "Total top-quark pair-production cross section at hadron colliders through $O(\alpha_S^4)$", *Phys. Rev. Lett.* **110** (2013) 252004, doi:10.1103/PhysRevLett.110.252004, arXiv:1303.6254.

[50] P. Kant et al., "HatHor for single top-quark production: Updated predictions and uncertainty estimates for single top-quark production in hadronic collisions", *Comput. Phys. Commun.* **191** (2015) 74, doi:10.1016/j.cpc.2015.02.001, arXiv:1406.4403.

[51] E. Re, "Single-top *Wt*-channel production matched with parton showers using the POWHEG method", *Eur. Phys. J. C* **71** (2011) 1547, doi:10.1140/epjc/s10052-011-1547-z, arXiv:1009.2450.

[52] J. Alwall et al., "The automated computation of tree-level and next-to-leading order differential cross sections, and their matching to parton shower simulations", *JHEP* **07** (2014) 079, doi:10.1007/JHEP07(2014)079, arXiv:1405.0301.

[53] R. Gavin, Y. Li, F. Petriello, and S. Quackenbush, "FEWZ 2.0: A code for hadronic Z production at next-to-next-to-leading order", *Comput. Phys. Commun.* **182** (2011) 2388, doi:10.1016/j.cpc.2011.06.008, arXiv:1011.3540.

[54] M. V. Garzelli, A. Kardos, C. G. Papadopoulos, and Z. Trocsanyi, "$t\bar{t}W^{\pm}$ and $t\bar{t}Z$ hadroproduction at NLO accuracy in QCD with parton shower and hadronization effects", *JHEP* **11** (2012) 056, doi:10.1007/JHEP11(2012)056, arXiv:1208.2665.

[55] T. Sjöstrand et al., "An introduction to PYTHIA 8.2", *Comput. Phys. Commun.* **191** (2015) 159, doi:10.1016/j.cpc.2015.01.024, arXiv:1410.3012.

[56] P. Skands, S. Carrazza, and J. Rojo, "Tuning PYTHIA 8.1: the Monash 2013 tune", *Eur. Phys. J. C* **74** (2014) 3024, doi:10.1140/epjc/s10052-014-3024-y, arXiv:1404.5630.

[57] CMS Collaboration, "Event generator tunes obtained from underlying event and multiparton scattering measurements", *Eur. Phys. J. C* **76** (2016) 155, doi:10.1140/epjc/s10052-016-3988-x, arXiv:1512.00815.

[58] NNPDF Collaboration, "Parton distributions for the LHC Run II", *JHEP* **04** (2015) 040, doi:10.1007/JHEP04(2015)040, arXiv:1410.8849.

[59] GEANT4 Collaboration, "GEANT4—a simulation toolkit", *Nucl. Instrum. Meth. A* **506** (2003) 250, doi:10.1016/S0168-9002(03)01368-8.

[60] C. Borschensky et al., "Squark and gluino production cross sections in pp collisions at $\sqrt{s}$ = 13, 14, 33 and 100 TeV", *Eur. Phys. J. C* **74** (2014) 3174, doi:10.1140/epjc/s10052-014-3174-y, arXiv:1407.5066.

[61] S. Abdullin et al., "The fast simulation of the CMS detector at LHC", *J. Phys. Conf. Ser.* **331** (2011) 032049, doi:10.1088/1742-6596/331/3/032049.

[62] CMS Collaboration, "Particle-flow reconstruction and global event description with the CMS detector", *JINST* **12** (2017) P10003, doi:10.1088/1748-0221/12/10/P10003, arXiv:1706.04965.

[63] CMS Collaboration, "Performance of electron reconstruction and selection with the CMS detector in proton-proton collisions at $\sqrt{s} = 8$ TeV", *JINST* **10** (2015) P06005, doi:10.1088/1748-0221/10/06/P06005, arXiv:1502.02701.

[64] CMS Collaboration, "Performance of CMS muon reconstruction in pp collision events at $\sqrt{s} = 7$ TeV", *JINST* **7** (2012) P10002, doi:10.1088/1748-0221/7/10/P10002, arXiv:1206.4071.

[65] M. Cacciari, G. P. Salam, and G. Soyez, "The anti-k_t jet clustering algorithm", *JHEP* **04** (2008) 063, doi:10.1088/1126-6708/2008/04/063, arXiv:0802.1189.

[66] M. Cacciari, G. P. Salam, and G. Soyez, "FastJet user manual", *Eur. Phys. J. C* **72** (2012) 1896, doi:10.1140/epjc/s10052-012-1896-2, arXiv:1111.6097.

[67] CMS Collaboration, "Jet energy scale and resolution in the CMS experiment in pp collisions at 8 TeV", *JINST* **12** (2017) P02014, doi:10.1088/1748-0221/12/02/P02014, arXiv:1607.03663.

[68] CMS Collaboration, "Performance of the CMS missing transverse momentum reconstruction in pp data at $\sqrt{s}$ = 8 TeV", *JINST* **10** (2015) P02006, doi:10.1088/1748-0221/10/02/P02006, arXiv:1411.0511.

[69] CMS Collaboration, "Identification of heavy-flavour jets with the CMS detector in pp collisions at 13 TeV", (2017). arXiv:1712.07158. Submitted to *JINST*.

[70] M. Burns, K. Kong, K. T. Matchev, and M. Park, "Using subsystem M_{T2} for complete mass determinations in decay chains with missing energy at hadron colliders", *JHEP* **03** (2009) 143, doi:10.1088/1126-6708/2009/03/143, arXiv:0810.5576.

[71] H.-C. Cheng and Z. Han, "Minimal kinematic constraints and m_{T2}", *JHEP* **12** (2008) 063, doi:10.1088/1126-6708/2008/12/063, arXiv:0810.5178.

[72] CMS Collaboration, "CMS luminosity measurement for the 2016 data taking period", CMS Physics Analysis Summary CMS-PAS-LUM-17-001, 2017.

[73] J. Butterworth et al., "PDF4LHC recommendations for LHC Run II", *J. Phys. G* **43** (2016) 023001, doi:10.1088/0954-3899/43/2/023001, arXiv:1510.03865.

[74] CMS Collaboration, "Measurement of the differential cross section for top quark pair production in pp collisions at $\sqrt{s} = 8$ TeV", *Eur. Phys. J. C* **75** (2015) 542, doi:10.1140/epjc/s10052-015-3709-x, arXiv:1505.04480.

[75] CMS Collaboration, "Measurement of differential cross sections for top quark pair production using the lepton+jets final state in proton-proton collisions at 13 TeV", *Phys. Rev. D* **95** (2017) 092001, doi:10.1103/PhysRevD.95.092001, arXiv:1610.04191.

[76] S. Catani, D. de Florian, M. Grazzini, and P. Nason, "Soft gluon resummation for Higgs boson production at hadron colliders", *JHEP* **07** (2003) 028, doi:10.1088/1126-6708/2003/07/028, arXiv:hep-ph/0306211.

[77] M. Cacciari et al., "The $\mathrm{t\bar{t}}$ cross-section at 1.8 TeV and 1.96 TeV: a study of the systematics due to parton densities and scale dependence", *JHEP* **04** (2004) 068, doi:10.1088/1126-6708/2004/04/068, arXiv:hep-ph/0303085.

[78] G. Cowan, K. Cranmer, E. Gross, and O. Vitells, "Asymptotic formulae for likelihood-based tests of new physics", *Eur. Phys. J. C* **71** (2011) 1554, doi:10.1140/epjc/s10052-011-1554-0, arXiv:1007.1727. [Erratum: doi:10.1140/epjc/s10052-013-2501-z].

[79] T. Junk, "Confidence level computation for combining searches with small statistics", *Nucl. Instr. Meth. A* **434** (1999) 435, doi:10.1016/S0168-9002(99)00498-2, arXiv:hep-ex/9902006.

[80] A. L. Read, "Presentation of search results: the CL_s technique", in *Durham IPPP Workshop: Advanced Statistical Techniques in Particle Physics*, p. 2693. Durham, UK, March, 2002. [J. Phys. G 28 (2002) 2693]. doi:10.1088/0954-3899/28/10/313.

[81] G. Belanger, R. M. Godbole, L. Hartgring, and I. Niessen, "Top polarization in stop production at the LHC", *JHEP* **05** (2013) 167, doi:10.1007/JHEP05(2013)167, arXiv:1212.3526.

[82] CMS Collaboration, "Simplified likelihood for the re-interpretation of public CMS results", Technical Report CERN-CMS-NOTE-2017-001, 2017.

A The CMS Collaboration

Yerevan Physics Institute, Yerevan, Armenia
A.M. Sirunyan, A. Tumasyan

Institut für Hochenergiephysik, Wien, Austria
W. Adam, F. Ambrogi, E. Asilar, T. Bergauer, J. Brandstetter, E. Brondolin, M. Dragicevic, J. Erö, M. Flechl, M. Friedl, R. Frühwirth[1], V.M. Ghete, J. Grossmann, J. Hrubec, M. Jeitler[1], A. König, N. Krammer, I. Krätschmer, D. Liko, T. Madlener, I. Mikulec, E. Pree, N. Rad, H. Rohringer, J. Schieck[1], R. Schöfbeck, M. Spanring, D. Spitzbart, W. Waltenberger, J. Wittmann, C.-E. Wulz[1], M. Zarucki

Institute for Nuclear Problems, Minsk, Belarus
V. Chekhovsky, V. Mossolov, J. Suarez Gonzalez

Universiteit Antwerpen, Antwerpen, Belgium
E.A. De Wolf, D. Di Croce, X. Janssen, J. Lauwers, M. Van De Klundert, H. Van Haevermaet, P. Van Mechelen, N. Van Remortel

Vrije Universiteit Brussel, Brussel, Belgium
S. Abu Zeid, F. Blekman, J. D'Hondt, I. De Bruyn, J. De Clercq, K. Deroover, G. Flouris, D. Lontkovskyi, S. Lowette, I. Marchesini, S. Moortgat, L. Moreels, Q. Python, K. Skovpen, S. Tavernier, W. Van Doninck, P. Van Mulders, I. Van Parijs

Université Libre de Bruxelles, Bruxelles, Belgium
D. Beghin, H. Brun, B. Clerbaux, G. De Lentdecker, H. Delannoy, B. Dorney, G. Fasanella, L. Favart, R. Goldouzian, A. Grebenyuk, T. Lenzi, J. Luetic, T. Maerschalk, A. Marinov, T. Seva, E. Starling, C. Vander Velde, P. Vanlaer, D. Vannerom, R. Yonamine, F. Zenoni, F. Zhang[2]

Ghent University, Ghent, Belgium
A. Cimmino, T. Cornelis, D. Dobur, A. Fagot, M. Gul, I. Khvastunov[3], D. Poyraz, C. Roskas, S. Salva, M. Tytgat, W. Verbeke, N. Zaganidis

Université Catholique de Louvain, Louvain-la-Neuve, Belgium
H. Bakhshiansohi, O. Bondu, S. Brochet, G. Bruno, C. Caputo, A. Caudron, P. David, S. De Visscher, C. Delaere, M. Delcourt, B. Francois, A. Giammanco, M. Komm, G. Krintiras, V. Lemaitre, A. Magitteri, A. Mertens, M. Musich, K. Piotrzkowski, L. Quertenmont, A. Saggio, M. Vidal Marono, S. Wertz, J. Zobec

Centro Brasileiro de Pesquisas Fisicas, Rio de Janeiro, Brazil
W.L. Aldá Júnior, F.L. Alves, G.A. Alves, L. Brito, M. Correa Martins Junior, C. Hensel, A. Moraes, M.E. Pol, P. Rebello Teles

Universidade do Estado do Rio de Janeiro, Rio de Janeiro, Brazil
E. Belchior Batista Das Chagas, W. Carvalho, J. Chinellato[4], E. Coelho, E.M. Da Costa, G.G. Da Silveira[5], D. De Jesus Damiao, S. Fonseca De Souza, L.M. Huertas Guativa, H. Malbouisson, M. Melo De Almeida, C. Mora Herrera, L. Mundim, H. Nogima, L.J. Sanchez Rosas, A. Santoro, A. Sznajder, M. Thiel, E.J. Tonelli Manganote[4], F. Torres Da Silva De Araujo, A. Vilela Pereira

Universidade Estadual Paulista [a], Universidade Federal do ABC [b], São Paulo, Brazil
S. Ahuja[a], C.A. Bernardes[a], T.R. Fernandez Perez Tomei[a], E.M. Gregores[b], P.G. Mercadante[b], S.F. Novaes[a], Sandra S. Padula[a], D. Romero Abad[b], J.C. Ruiz Vargas[a]

Institute for Nuclear Research and Nuclear Energy, Bulgarian Academy of Sciences, Sofia, Bulgaria
A. Aleksandrov, R. Hadjiiska, P. Iaydjiev, M. Misheva, M. Rodozov, M. Shopova, G. Sultanov

University of Sofia, Sofia, Bulgaria
A. Dimitrov, L. Litov, B. Pavlov, P. Petkov

Beihang University, Beijing, China
W. Fang[6], X. Gao[6], L. Yuan

Institute of High Energy Physics, Beijing, China
M. Ahmad, J.G. Bian, G.M. Chen, H.S. Chen, M. Chen, Y. Chen, C.H. Jiang, D. Leggat, H. Liao, Z. Liu, F. Romeo, S.M. Shaheen, A. Spiezia, J. Tao, C. Wang, Z. Wang, E. Yazgan, H. Zhang, S. Zhang, J. Zhao

State Key Laboratory of Nuclear Physics and Technology, Peking University, Beijing, China
Y. Ban, G. Chen, Q. Li, S. Liu, Y. Mao, S.J. Qian, D. Wang, Z. Xu

Universidad de Los Andes, Bogota, Colombia
C. Avila, A. Cabrera, L.F. Chaparro Sierra, C. Florez, C.F. González Hernández, J.D. Ruiz Alvarez, M.A. Segura Delgado

University of Split, Faculty of Electrical Engineering, Mechanical Engineering and Naval Architecture, Split, Croatia
B. Courbon, N. Godinovic, D. Lelas, I. Puljak, P.M. Ribeiro Cipriano, T. Sculac

University of Split, Faculty of Science, Split, Croatia
Z. Antunovic, M. Kovac

Institute Rudjer Boskovic, Zagreb, Croatia
V. Brigljevic, D. Ferencek, K. Kadija, B. Mesic, A. Starodumov[7], T. Susa

University of Cyprus, Nicosia, Cyprus
M.W. Ather, A. Attikis, G. Mavromanolakis, J. Mousa, C. Nicolaou, F. Ptochos, P.A. Razis, H. Rykaczewski

Charles University, Prague, Czech Republic
M. Finger[8], M. Finger Jr.[8]

Universidad San Francisco de Quito, Quito, Ecuador
E. Carrera Jarrin

Academy of Scientific Research and Technology of the Arab Republic of Egypt, Egyptian Network of High Energy Physics, Cairo, Egypt
E. El-khateeb[9], S. Elgammal[10], A. Mohamed[11]

National Institute of Chemical Physics and Biophysics, Tallinn, Estonia
R.K. Dewanjee, M. Kadastik, L. Perrini, M. Raidal, A. Tiko, C. Veelken

Department of Physics, University of Helsinki, Helsinki, Finland
P. Eerola, H. Kirschenmann, J. Pekkanen, M. Voutilainen

Helsinki Institute of Physics, Helsinki, Finland
J. Havukainen, J.K. Heikkilä, T. Järvinen, V. Karimäki, R. Kinnunen, T. Lampén, K. Lassila-Perini, S. Laurila, S. Lehti, T. Lindén, P. Luukka, H. Siikonen, E. Tuominen, J. Tuominiemi

Lappeenranta University of Technology, Lappeenranta, Finland
T. Tuuva

IRFU, CEA, Université Paris-Saclay, Gif-sur-Yvette, France
M. Besancon, F. Couderc, M. Dejardin, D. Denegri, J.L. Faure, F. Ferri, S. Ganjour, S. Ghosh, P. Gras, G. Hamel de Monchenault, P. Jarry, I. Kucher, C. Leloup, E. Locci, M. Machet, J. Malcles, G. Negro, J. Rander, A. Rosowsky, M.Ö. Sahin, M. Titov

Laboratoire Leprince-Ringuet, Ecole polytechnique, CNRS/IN2P3, Université Paris-Saclay, Palaiseau, France
A. Abdulsalam, C. Amendola, I. Antropov, S. Baffioni, F. Beaudette, P. Busson, L. Cadamuro, C. Charlot, R. Granier de Cassagnac, M. Jo, S. Lisniak, A. Lobanov, J. Martin Blanco, M. Nguyen, C. Ochando, G. Ortona, P. Paganini, P. Pigard, R. Salerno, J.B. Sauvan, Y. Sirois, A.G. Stahl Leiton, T. Strebler, Y. Yilmaz, A. Zabi, A. Zghiche

Université de Strasbourg, CNRS, IPHC UMR 7178, F-67000 Strasbourg, France
J.-L. Agram[12], J. Andrea, D. Bloch, J.-M. Brom, M. Buttignol, E.C. Chabert, N. Chanon, C. Collard, E. Conte[12], X. Coubez, J.-C. Fontaine[12], D. Gelé, U. Goerlach, M. Jansová, A.-C. Le Bihan, N. Tonon, P. Van Hove

Centre de Calcul de l'Institut National de Physique Nucleaire et de Physique des Particules, CNRS/IN2P3, Villeurbanne, France
S. Gadrat

Université de Lyon, Université Claude Bernard Lyon 1, CNRS-IN2P3, Institut de Physique Nucléaire de Lyon, Villeurbanne, France
S. Beauceron, C. Bernet, G. Boudoul, R. Chierici, D. Contardo, P. Depasse, H. El Mamouni, J. Fay, L. Finco, S. Gascon, M. Gouzevitch, G. Grenier, B. Ille, F. Lagarde, I.B. Laktineh, M. Lethuillier, L. Mirabito, A.L. Pequegnot, S. Perries, A. Popov[13], V. Sordini, M. Vander Donckt, S. Viret

Georgian Technical University, Tbilisi, Georgia
A. Khvedelidze[8]

Tbilisi State University, Tbilisi, Georgia
Z. Tsamalaidze[8]

RWTH Aachen University, I. Physikalisches Institut, Aachen, Germany
C. Autermann, L. Feld, M.K. Kiesel, K. Klein, M. Lipinski, M. Preuten, C. Schomakers, J. Schulz, V. Zhukov[13]

RWTH Aachen University, III. Physikalisches Institut A, Aachen, Germany
A. Albert, E. Dietz-Laursonn, D. Duchardt, M. Endres, M. Erdmann, S. Erdweg, T. Esch, R. Fischer, A. Güth, M. Hamer, T. Hebbeker, C. Heidemann, K. Hoepfner, S. Knutzen, M. Merschmeyer, A. Meyer, P. Millet, S. Mukherjee, T. Pook, M. Radziej, H. Reithler, M. Rieger, F. Scheuch, D. Teyssier, S. Thüer

RWTH Aachen University, III. Physikalisches Institut B, Aachen, Germany
G. Flügge, B. Kargoll, T. Kress, A. Künsken, T. Müller, A. Nehrkorn, A. Nowack, C. Pistone, O. Pooth, A. Stahl[14]

Deutsches Elektronen-Synchrotron, Hamburg, Germany
M. Aldaya Martin, T. Arndt, C. Asawatangtrakuldee, K. Beernaert, O. Behnke, U. Behrens, A. Bermúdez Martínez, A.A. Bin Anuar, K. Borras[15], V. Botta, A. Campbell, P. Connor, C. Contreras-Campana, F. Costanza, C. Diez Pardos, G. Eckerlin, D. Eckstein, T. Eichhorn,

E. Eren, E. Gallo[16], J. Garay Garcia, A. Geiser, J.M. Grados Luyando, A. Grohsjean, P. Gunnellini, M. Guthoff, A. Harb, J. Hauk, M. Hempel[17], H. Jung, M. Kasemann, J. Keaveney, C. Kleinwort, I. Korol, D. Krücker, W. Lange, A. Lelek, T. Lenz, J. Leonard, K. Lipka, W. Lohmann[17], R. Mankel, I.-A. Melzer-Pellmann, A.B. Meyer, G. Mittag, J. Mnich, A. Mussgiller, E. Ntomari, D. Pitzl, A. Raspereza, M. Savitskyi, P. Saxena, R. Shevchenko, S. Spannagel, N. Stefaniuk, G.P. Van Onsem, R. Walsh, Y. Wen, K. Wichmann, C. Wissing, O. Zenaiev

University of Hamburg, Hamburg, Germany
R. Aggleton, S. Bein, V. Blobel, M. Centis Vignali, T. Dreyer, E. Garutti, D. Gonzalez, J. Haller, A. Hinzmann, M. Hoffmann, A. Karavdina, R. Klanner, R. Kogler, N. Kovalchuk, S. Kurz, T. Lapsien, D. Marconi, M. Meyer, M. Niedziela, D. Nowatschin, F. Pantaleo[14], T. Peiffer, A. Perieanu, C. Scharf, P. Schleper, A. Schmidt, S. Schumann, J. Schwandt, J. Sonneveld, H. Stadie, G. Steinbrück, F.M. Stober, M. Stöver, H. Tholen, D. Troendle, E. Usai, A. Vanhoefer, B. Vormwald

Institut für Experimentelle Kernphysik, Karlsruhe, Germany
M. Akbiyik, C. Barth, M. Baselga, S. Baur, E. Butz, R. Caspart, T. Chwalek, F. Colombo, W. De Boer, A. Dierlamm, N. Faltermann, B. Freund, R. Friese, M. Giffels, M.A. Harrendorf, F. Hartmann[14], S.M. Heindl, U. Husemann, F. Kassel[14], S. Kudella, H. Mildner, M.U. Mozer, Th. Müller, M. Plagge, G. Quast, K. Rabbertz, M. Schröder, I. Shvetsov, G. Sieber, H.J. Simonis, R. Ulrich, S. Wayand, M. Weber, T. Weiler, S. Williamson, C. Wöhrmann, R. Wolf

Institute of Nuclear and Particle Physics (INPP), NCSR Demokritos, Aghia Paraskevi, Greece
G. Anagnostou, G. Daskalakis, T. Geralis, A. Kyriakis, D. Loukas, I. Topsis-Giotis

National and Kapodistrian University of Athens, Athens, Greece
G. Karathanasis, S. Kesisoglou, A. Panagiotou, N. Saoulidou

National Technical University of Athens, Athens, Greece
K. Kousouris

University of Ioánnina, Ioánnina, Greece
I. Evangelou, C. Foudas, P. Kokkas, S. Mallios, N. Manthos, I. Papadopoulos, E. Paradas, J. Strologas, F.A. Triantis

MTA-ELTE Lendület CMS Particle and Nuclear Physics Group, Eötvös Loránd University, Budapest, Hungary
M. Csanad, N. Filipovic, G. Pasztor, O. Surányi, G.I. Veres[18]

Wigner Research Centre for Physics, Budapest, Hungary
G. Bencze, C. Hajdu, D. Horvath[19], Á. Hunyadi, F. Sikler, V. Veszpremi

Institute of Nuclear Research ATOMKI, Debrecen, Hungary
N. Beni, S. Czellar, J. Karancsi[20], A. Makovec, J. Molnar, Z. Szillasi

Institute of Physics, University of Debrecen, Debrecen, Hungary
M. Bartók[18], P. Raics, Z.L. Trocsanyi, B. Ujvari

Indian Institute of Science (IISc), Bangalore, India
S. Choudhury, J.R. Komaragiri

National Institute of Science Education and Research, Bhubaneswar, India
S. Bahinipati[21], S. Bhowmik, P. Mal, K. Mandal, A. Nayak[22], D.K. Sahoo[21], N. Sahoo, S.K. Swain

Panjab University, Chandigarh, India
S. Bansal, S.B. Beri, V. Bhatnagar, R. Chawla, N. Dhingra, A.K. Kalsi, A. Kaur, M. Kaur, S. Kaur, R. Kumar, P. Kumari, A. Mehta, J.B. Singh, G. Walia

University of Delhi, Delhi, India
Ashok Kumar, Aashaq Shah, A. Bhardwaj, S. Chauhan, B.C. Choudhary, R.B. Garg, S. Keshri, A. Kumar, S. Malhotra, M. Naimuddin, K. Ranjan, R. Sharma

Saha Institute of Nuclear Physics, HBNI, Kolkata, India
R. Bhardwaj, R. Bhattacharya, S. Bhattacharya, U. Bhawandeep, S. Dey, S. Dutt, S. Dutta, S. Ghosh, N. Majumdar, A. Modak, K. Mondal, S. Mukhopadhyay, S. Nandan, A. Purohit, A. Roy, S. Roy Chowdhury, S. Sarkar, M. Sharan, S. Thakur

Indian Institute of Technology Madras, Madras, India
P.K. Behera

Bhabha Atomic Research Centre, Mumbai, India
R. Chudasama, D. Dutta, V. Jha, V. Kumar, A.K. Mohanty[14], P.K. Netrakanti, L.M. Pant, P. Shukla, A. Topkar

Tata Institute of Fundamental Research-A, Mumbai, India
T. Aziz, S. Dugad, B. Mahakud, S. Mitra, G.B. Mohanty, N. Sur, B. Sutar

Tata Institute of Fundamental Research-B, Mumbai, India
S. Banerjee, S. Bhattacharya, S. Chatterjee, P. Das, M. Guchait, Sa. Jain, S. Kumar, M. Maity[23], G. Majumder, K. Mazumdar, T. Sarkar[23], N. Wickramage[24]

Indian Institute of Science Education and Research (IISER), Pune, India
S. Chauhan, S. Dube, V. Hegde, A. Kapoor, K. Kothekar, S. Pandey, A. Rane, S. Sharma

Institute for Research in Fundamental Sciences (IPM), Tehran, Iran
S. Chenarani[25], E. Eskandari Tadavani, S.M. Etesami[25], M. Khakzad, M. Mohammadi Najafabadi, M. Naseri, S. Paktinat Mehdiabadi[26], F. Rezaei Hosseinabadi, B. Safarzadeh[27], M. Zeinali

University College Dublin, Dublin, Ireland
M. Felcini, M. Grunewald

INFN Sezione di Bari [a], Università di Bari [b], Politecnico di Bari [c], Bari, Italy
M. Abbrescia[a,b], C. Calabria[a,b], A. Colaleo[a], D. Creanza[a,c], L. Cristella[a,b], N. De Filippis[a,c], M. De Palma[a,b], F. Errico[a,b], L. Fiore[a], G. Iaselli[a,c], S. Lezki[a,b], G. Maggi[a,c], M. Maggi[a], G. Miniello[a,b], S. My[a,b], S. Nuzzo[a,b], A. Pompili[a,b], G. Pugliese[a,c], R. Radogna[a], A. Ranieri[a], G. Selvaggi[a,b], A. Sharma[a], L. Silvestris[a,14], R. Venditti[a], P. Verwilligen[a]

INFN Sezione di Bologna [a], Università di Bologna [b], Bologna, Italy
G. Abbiendi[a], C. Battilana[a,b], D. Bonacorsi[a,b], L. Borgonovi[a,b], S. Braibant-Giacomelli[a,b], R. Campanini[a,b], P. Capiluppi[a,b], A. Castro[a,b], F.R. Cavallo[a], S.S. Chhibra[a], G. Codispoti[a,b], M. Cuffiani[a,b], G.M. Dallavalle[a], F. Fabbri[a], A. Fanfani[a,b], D. Fasanella[a,b], P. Giacomelli[a], C. Grandi[a], L. Guiducci[a,b], S. Marcellini[a], G. Masetti[a], A. Montanari[a], F.L. Navarria[a,b], A. Perrotta[a], A.M. Rossi[a,b], T. Rovelli[a,b], G.P. Siroli[a,b], N. Tosi[a]

INFN Sezione di Catania [a], Università di Catania [b], Catania, Italy
S. Albergo[a,b], S. Costa[a,b], A. Di Mattia[a], F. Giordano[a,b], R. Potenza[a,b], A. Tricomi[a,b], C. Tuve[a,b]

INFN Sezione di Firenze [a], Università di Firenze [b], Firenze, Italy
G. Barbagli[a], K. Chatterjee[a,b], V. Ciulli[a,b], C. Civinini[a], R. D'Alessandro[a,b], E. Focardi[a,b], P. Lenzi[a,b], M. Meschini[a], S. Paoletti[a], L. Russo[a,28], G. Sguazzoni[a], D. Strom[a], L. Viliani[a,b,14]

INFN Laboratori Nazionali di Frascati, Frascati, Italy
L. Benussi, S. Bianco, F. Fabbri, D. Piccolo, F. Primavera[14]

INFN Sezione di Genova [a], Università di Genova [b], Genova, Italy
V. Calvelli[a,b], F. Ferro[a], E. Robutti[a], S. Tosi[a,b]

INFN Sezione di Milano-Bicocca [a], Università di Milano-Bicocca [b], Milano, Italy
A. Benaglia[a], A. Beschi[b], L. Brianza[a,b], F. Brivio[a,b], V. Ciriolo[a,b,14], M.E. Dinardo[a,b], S. Fiorendi[a,b], S. Gennai[a], A. Ghezzi[a,b], P. Govoni[a,b], M. Malberti[a,b], S. Malvezzi[a], R.A. Manzoni[a,b], D. Menasce[a], L. Moroni[a], M. Paganoni[a,b], K. Pauwels[a,b], D. Pedrini[a], S. Pigazzini[a,b,29], S. Ragazzi[a,b], T. Tabarelli de Fatis[a,b]

INFN Sezione di Napoli [a], Università di Napoli 'Federico II' [b], Napoli, Italy, Università della Basilicata [c], Potenza, Italy, Università G. Marconi [d], Roma, Italy
S. Buontempo[a], N. Cavallo[a,c], S. Di Guida[a,d,14], F. Fabozzi[a,c], F. Fienga[a,b], A.O.M. Iorio[a,b], W.A. Khan[a], L. Lista[a], S. Meola[a,d,14], P. Paolucci[a,14], C. Sciacca[a,b], F. Thyssen[a]

INFN Sezione di Padova [a], Università di Padova [b], Padova, Italy, Università di Trento [c], Trento, Italy
P. Azzi[a], N. Bacchetta[a], L. Benato[a,b], D. Bisello[a,b], A. Boletti[a,b], R. Carlin[a,b], A. Carvalho Antunes De Oliveira[a,b], P. Checchia[a], M. Dall'Osso[a,b], P. De Castro Manzano[a], T. Dorigo[a], U. Dosselli[a], F. Gasparini[a,b], U. Gasparini[a,b], S. Lacaprara[a], P. Lujan, A.T. Meneguzzo[a,b], D. Pantano[a], N. Pozzobon[a,b], P. Ronchese[a,b], R. Rossin[a,b], F. Simonetto[a,b], E. Torassa[a], M. Zanetti[a,b], P. Zotto[a,b], G. Zumerle[a,b]

INFN Sezione di Pavia [a], Università di Pavia [b], Pavia, Italy
A. Braghieri[a], A. Magnani[a], P. Montagna[a,b], S.P. Ratti[a,b], V. Re[a], M. Ressegotti[a,b], C. Riccardi[a,b], P. Salvini[a], I. Vai[a,b], P. Vitulo[a,b]

INFN Sezione di Perugia [a], Università di Perugia [b], Perugia, Italy
L. Alunni Solestizi[a,b], M. Biasini[a,b], G.M. Bilei[a], C. Cecchi[a,b], D. Ciangottini[a,b], L. Fanò[a,b], P. Lariccia[a,b], R. Leonardi[a,b], E. Manoni[a], G. Mantovani[a,b], V. Mariani[a,b], M. Menichelli[a], A. Rossi[a,b], A. Santocchia[a,b], D. Spiga[a]

INFN Sezione di Pisa [a], Università di Pisa [b], Scuola Normale Superiore di Pisa [c], Pisa, Italy
K. Androsov[a], P. Azzurri[a,14], G. Bagliesi[a], T. Boccali[a], L. Borrello, R. Castaldi[a], M.A. Ciocci[a,b], R. Dell'Orso[a], G. Fedi[a], L. Giannini[a,c], A. Giassi[a], M.T. Grippo[a,28], F. Ligabue[a,c], T. Lomtadze[a], E. Manca[a,c], G. Mandorli[a,c], A. Messineo[a,b], F. Palla[a], A. Rizzi[a,b], A. Savoy-Navarro[a,30], P. Spagnolo[a], R. Tenchini[a], G. Tonelli[a,b], A. Venturi[a], P.G. Verdini[a]

INFN Sezione di Roma [a], Sapienza Università di Roma [b], Rome, Italy
L. Barone[a,b], F. Cavallari[a], M. Cipriani[a,b], N. Daci[a], D. Del Re[a,b,14], E. Di Marco[a,b], M. Diemoz[a], S. Gelli[a,b], E. Longo[a,b], F. Margaroli[a,b], B. Marzocchi[a,b], P. Meridiani[a], G. Organtini[a,b], R. Paramatti[a,b], F. Preiato[a,b], S. Rahatlou[a,b], C. Rovelli[a], F. Santanastasio[a,b]

INFN Sezione di Torino [a], Università di Torino [b], Torino, Italy, Università del Piemonte Orientale [c], Novara, Italy
N. Amapane[a,b], R. Arcidiacono[a,c], S. Argiro[a,b], M. Arneodo[a,c], N. Bartosik[a], R. Bellan[a,b], C. Biino[a], N. Cartiglia[a], F. Cenna[a,b], M. Costa[a,b], R. Covarelli[a,b], A. Degano[a,b], N. Demaria[a], B. Kiani[a,b], C. Mariotti[a], S. Maselli[a], E. Migliore[a,b], V. Monaco[a,b], E. Monteil[a,b], M. Monteno[a],

M.M. Obertino[a,b], L. Pacher[a,b], N. Pastrone[a], M. Pelliccioni[a], G.L. Pinna Angioni[a,b], F. Ravera[a,b], A. Romero[a,b], M. Ruspa[a,c], R. Sacchi[a,b], K. Shchelina[a,b], V. Sola[a], A. Solano[a,b], A. Staiano[a], P. Traczyk[a,b]

INFN Sezione di Trieste [a], Università di Trieste [b], Trieste, Italy
S. Belforte[a], M. Casarsa[a], F. Cossutti[a], G. Della Ricca[a,b], A. Zanetti[a]

Kyungpook National University, Daegu, Korea
D.H. Kim, G.N. Kim, M.S. Kim, J. Lee, S. Lee, S.W. Lee, C.S. Moon, Y.D. Oh, S. Sekmen, D.C. Son, Y.C. Yang

Chonbuk National University, Jeonju, Korea
A. Lee

Chonnam National University, Institute for Universe and Elementary Particles, Kwangju, Korea
H. Kim, D.H. Moon, G. Oh

Hanyang University, Seoul, Korea
J.A. Brochero Cifuentes, J. Goh, T.J. Kim

Korea University, Seoul, Korea
S. Cho, S. Choi, Y. Go, D. Gyun, S. Ha, B. Hong, Y. Jo, Y. Kim, K. Lee, K.S. Lee, S. Lee, J. Lim, S.K. Park, Y. Roh

Seoul National University, Seoul, Korea
J. Almond, J. Kim, J.S. Kim, H. Lee, K. Lee, K. Nam, S.B. Oh, B.C. Radburn-Smith, S.h. Seo, U.K. Yang, H.D. Yoo, G.B. Yu

University of Seoul, Seoul, Korea
H. Kim, J.H. Kim, J.S.H. Lee, I.C. Park

Sungkyunkwan University, Suwon, Korea
Y. Choi, C. Hwang, J. Lee, I. Yu

Vilnius University, Vilnius, Lithuania
V. Dudenas, A. Juodagalvis, J. Vaitkus

National Centre for Particle Physics, Universiti Malaya, Kuala Lumpur, Malaysia
I. Ahmed, Z.A. Ibrahim, M.A.B. Md Ali[31], F. Mohamad Idris[32], W.A.T. Wan Abdullah, M.N. Yusli, Z. Zolkapli

Centro de Investigacion y de Estudios Avanzados del IPN, Mexico City, Mexico
Reyes-Almanza, R, Ramirez-Sanchez, G., Duran-Osuna, M. C., H. Castilla-Valdez, E. De La Cruz-Burelo, I. Heredia-De La Cruz[33], Rabadan-Trejo, R. I., R. Lopez-Fernandez, J. Mejia Guisao, A. Sanchez-Hernandez

Universidad Iberoamericana, Mexico City, Mexico
S. Carrillo Moreno, C. Oropeza Barrera, F. Vazquez Valencia

Benemerita Universidad Autonoma de Puebla, Puebla, Mexico
I. Pedraza, H.A. Salazar Ibarguen, C. Uribe Estrada

Universidad Autónoma de San Luis Potosí, San Luis Potosí, Mexico
A. Morelos Pineda

University of Auckland, Auckland, New Zealand
D. Krofcheck

University of Canterbury, Christchurch, New Zealand
P.H. Butler

National Centre for Physics, Quaid-I-Azam University, Islamabad, Pakistan
A. Ahmad, M. Ahmad, Q. Hassan, H.R. Hoorani, A. Saddique, M.A. Shah, M. Shoaib, M. Waqas

National Centre for Nuclear Research, Swierk, Poland
H. Bialkowska, M. Bluj, B. Boimska, T. Frueboes, M. Górski, M. Kazana, K. Nawrocki, M. Szleper, P. Zalewski

Institute of Experimental Physics, Faculty of Physics, University of Warsaw, Warsaw, Poland
K. Bunkowski, A. Byszuk[34], K. Doroba, A. Kalinowski, M. Konecki, J. Krolikowski, M. Misiura, M. Olszewski, A. Pyskir, M. Walczak

Laboratório de Instrumentação e Física Experimental de Partículas, Lisboa, Portugal
P. Bargassa, C. Beirão Da Cruz E Silva, A. Di Francesco, P. Faccioli, B. Galinhas, M. Gallinaro, J. Hollar, N. Leonardo, L. Lloret Iglesias, M.V. Nemallapudi, J. Seixas, G. Strong, O. Toldaiev, D. Vadruccio, J. Varela

Joint Institute for Nuclear Research, Dubna, Russia
V. Alexakhin, A. Golunov, I. Golutvin, N. Gorbounov, I. Gorbunov, A. Kamenev, V. Karjavin, A. Lanev, A. Malakhov, V. Matveev[35,36], V. Palichik, V. Perelygin, M. Savina, S. Shmatov, S. Shulha, N. Skatchkov, V. Smirnov, A. Zarubin

Petersburg Nuclear Physics Institute, Gatchina (St. Petersburg), Russia
Y. Ivanov, V. Kim[37], E. Kuznetsova[38], P. Levchenko, V. Murzin, V. Oreshkin, I. Smirnov, V. Sulimov, L. Uvarov, S. Vavilov, A. Vorobyev

Institute for Nuclear Research, Moscow, Russia
Yu. Andreev, A. Dermenev, S. Gninenko, N. Golubev, A. Karneyeu, M. Kirsanov, N. Krasnikov, A. Pashenkov, D. Tlisov, A. Toropin

Institute for Theoretical and Experimental Physics, Moscow, Russia
V. Epshteyn, V. Gavrilov, N. Lychkovskaya, V. Popov, I. Pozdnyakov, G. Safronov, A. Spiridonov, A. Stepennov, M. Toms, E. Vlasov, A. Zhokin

Moscow Institute of Physics and Technology, Moscow, Russia
T. Aushev, A. Bylinkin[36]

National Research Nuclear University 'Moscow Engineering Physics Institute' (MEPhI), Moscow, Russia
R. Chistov[39], M. Danilov[39], P. Parygin, D. Philippov, S. Polikarpov, E. Tarkovskii

P.N. Lebedev Physical Institute, Moscow, Russia
V. Andreev, M. Azarkin[36], I. Dremin[36], M. Kirakosyan[36], A. Terkulov

Skobeltsyn Institute of Nuclear Physics, Lomonosov Moscow State University, Moscow, Russia
A. Baskakov, A. Belyaev, E. Boos, V. Bunichev, M. Dubinin[40], L. Dudko, A. Ershov, A. Gribushin, V. Klyukhin, O. Kodolova, I. Lokhtin, I. Miagkov, S. Obraztsov, S. Petrushanko, V. Savrin

Novosibirsk State University (NSU), Novosibirsk, Russia
V. Blinov[41], Y.Skovpen[41], D. Shtol[41]

State Research Center of Russian Federation, Institute for High Energy Physics, Protvino, Russia
I. Azhgirey, I. Bayshev, S. Bitioukov, D. Elumakhov, V. Kachanov, A. Kalinin, D. Konstantinov, P. Mandrik, V. Petrov, R. Ryutin, A. Sobol, S. Troshin, N. Tyurin, A. Uzunian, A. Volkov

University of Belgrade, Faculty of Physics and Vinca Institute of Nuclear Sciences, Belgrade, Serbia
P. Adzic[42], P. Cirkovic, D. Devetak, M. Dordevic, J. Milosevic, V. Rekovic

Centro de Investigaciones Energéticas Medioambientales y Tecnológicas (CIEMAT), Madrid, Spain
J. Alcaraz Maestre, M. Barrio Luna, M. Cerrada, N. Colino, B. De La Cruz, A. Delgado Peris, A. Escalante Del Valle, C. Fernandez Bedoya, J.P. Fernández Ramos, J. Flix, M.C. Fouz, O. Gonzalez Lopez, S. Goy Lopez, J.M. Hernandez, M.I. Josa, D. Moran, A. Pérez-Calero Yzquierdo, J. Puerta Pelayo, A. Quintario Olmeda, I. Redondo, L. Romero, M.S. Soares, A. Álvarez Fernández

Universidad Autónoma de Madrid, Madrid, Spain
C. Albajar, J.F. de Trocóniz, M. Missiroli

Universidad de Oviedo, Oviedo, Spain
J. Cuevas, C. Erice, J. Fernandez Menendez, I. Gonzalez Caballero, J.R. González Fernández, E. Palencia Cortezon, S. Sanchez Cruz, P. Vischia, J.M. Vizan Garcia

Instituto de Física de Cantabria (IFCA), CSIC-Universidad de Cantabria, Santander, Spain
I.J. Cabrillo, A. Calderon, B. Chazin Quero, E. Curras, J. Duarte Campderros, M. Fernandez, J. Garcia-Ferrero, G. Gomez, A. Lopez Virto, J. Marco, C. Martinez Rivero, P. Martinez Ruiz del Arbol, F. Matorras, J. Piedra Gomez, T. Rodrigo, A. Ruiz-Jimeno, L. Scodellaro, N. Trevisani, I. Vila, R. Vilar Cortabitarte

CERN, European Organization for Nuclear Research, Geneva, Switzerland
D. Abbaneo, B. Akgun, E. Auffray, P. Baillon, A.H. Ball, D. Barney, J. Bendavid, M. Bianco, P. Bloch, A. Bocci, C. Botta, T. Camporesi, R. Castello, M. Cepeda, G. Cerminara, E. Chapon, Y. Chen, D. d'Enterria, A. Dabrowski, V. Daponte, A. David, M. De Gruttola, A. De Roeck, N. Deelen, M. Dobson, T. du Pree, M. Dünser, N. Dupont, A. Elliott-Peisert, P. Everaerts, F. Fallavollita, G. Franzoni, J. Fulcher, W. Funk, D. Gigi, A. Gilbert, K. Gill, F. Glege, D. Gulhan, P. Harris, J. Hegeman, V. Innocente, A. Jafari, P. Janot, O. Karacheban[17], J. Kieseler, V. Knünz, A. Kornmayer, M.J. Kortelainen, M. Krammer[1], C. Lange, P. Lecoq, C. Lourenço, M.T. Lucchini, L. Malgeri, M. Mannelli, A. Martelli, F. Meijers, J.A. Merlin, S. Mersi, E. Meschi, P. Milenovic[43], F. Moortgat, M. Mulders, H. Neugebauer, J. Ngadiuba, S. Orfanelli, L. Orsini, L. Pape, E. Perez, M. Peruzzi, A. Petrilli, G. Petrucciani, A. Pfeiffer, M. Pierini, D. Rabady, A. Racz, T. Reis, G. Rolandi[44], M. Rovere, H. Sakulin, C. Schäfer, C. Schwick, M. Seidel, M. Selvaggi, A. Sharma, P. Silva, P. Sphicas[45], A. Stakia, J. Steggemann, M. Stoye, M. Tosi, D. Treille, A. Triossi, A. Tsirou, V. Veckalns[46], M. Verweij, W.D. Zeuner

Paul Scherrer Institut, Villigen, Switzerland
W. Bertl[†], L. Caminada[47], K. Deiters, W. Erdmann, R. Horisberger, Q. Ingram, H.C. Kaestli, D. Kotlinski, U. Langenegger, T. Rohe, S.A. Wiederkehr

ETH Zurich - Institute for Particle Physics and Astrophysics (IPA), Zurich, Switzerland
M. Backhaus, L. Bäni, P. Berger, L. Bianchini, B. Casal, G. Dissertori, M. Dittmar, M. Donegà, C. Dorfer, C. Grab, C. Heidegger, D. Hits, J. Hoss, G. Kasieczka, T. Klijnsma, W. Lustermann,

B. Mangano, M. Marionneau, M.T. Meinhard, D. Meister, F. Micheli, P. Musella, F. Nessi-Tedaldi, F. Pandolfi, J. Pata, F. Pauss, G. Perrin, L. Perrozzi, M. Quittnat, M. Reichmann, D.A. Sanz Becerra, M. Schönenberger, L. Shchutska, V.R. Tavolaro, K. Theofilatos, M.L. Vesterbacka Olsson, R. Wallny, D.H. Zhu

Universität Zürich, Zurich, Switzerland
T.K. Aarrestad, C. Amsler[48], M.F. Canelli, A. De Cosa, R. Del Burgo, S. Donato, C. Galloni, T. Hreus, B. Kilminster, D. Pinna, G. Rauco, P. Robmann, D. Salerno, K. Schweiger, C. Seitz, Y. Takahashi, A. Zucchetta

National Central University, Chung-Li, Taiwan
V. Candelise, T.H. Doan, Sh. Jain, R. Khurana, C.M. Kuo, W. Lin, A. Pozdnyakov, S.S. Yu

National Taiwan University (NTU), Taipei, Taiwan
Arun Kumar, P. Chang, Y. Chao, K.F. Chen, P.H. Chen, F. Fiori, W.-S. Hou, Y. Hsiung, Y.F. Liu, R.-S. Lu, E. Paganis, A. Psallidas, A. Steen, J.f. Tsai

Chulalongkorn University, Faculty of Science, Department of Physics, Bangkok, Thailand
B. Asavapibhop, K. Kovitanggoon, G. Singh, N. Srimanobhas

Çukurova University, Physics Department, Science and Art Faculty, Adana, Turkey
M.N. Bakirci[49], A. Bat, F. Boran, S. Cerci[50], S. Damarseckin, Z.S. Demiroglu, C. Dozen, S. Girgis, G. Gokbulut, Y. Guler, I. Hos[51], E.E. Kangal[52], O. Kara, U. Kiminsu, M. Oglakci, G. Onengut[53], K. Ozdemir[54], S. Ozturk[49], A. Polatoz, U.G. Tok, H. Topakli[49], S. Turkcapar, I.S. Zorbakir, C. Zorbilmez

Middle East Technical University, Physics Department, Ankara, Turkey
B. Bilin, G. Karapinar[55], K. Ocalan[56], M. Yalvac, M. Zeyrek

Bogazici University, Istanbul, Turkey
E. Gülmez, M. Kaya[57], O. Kaya[58], S. Tekten, E.A. Yetkin[59]

Istanbul Technical University, Istanbul, Turkey
M.N. Agaras, S. Atay, A. Cakir, K. Cankocak, I. Köseoglu

Institute for Scintillation Materials of National Academy of Science of Ukraine, Kharkov, Ukraine
B. Grynyov

National Scientific Center, Kharkov Institute of Physics and Technology, Kharkov, Ukraine
L. Levchuk

University of Bristol, Bristol, United Kingdom
F. Ball, L. Beck, J.J. Brooke, D. Burns, E. Clement, D. Cussans, O. Davignon, H. Flacher, J. Goldstein, G.P. Heath, H.F. Heath, L. Kreczko, D.M. Newbold[60], S. Paramesvaran, T. Sakuma, S. Seif El Nasr-storey, D. Smith, V.J. Smith

Rutherford Appleton Laboratory, Didcot, United Kingdom
K.W. Bell, A. Belyaev[61], C. Brew, R.M. Brown, L. Calligaris, D. Cieri, D.J.A. Cockerill, J.A. Coughlan, K. Harder, S. Harper, J. Linacre, E. Olaiya, D. Petyt, C.H. Shepherd-Themistocleous, A. Thea, I.R. Tomalin, T. Williams

Imperial College, London, United Kingdom
G. Auzinger, R. Bainbridge, J. Borg, S. Breeze, O. Buchmuller, A. Bundock, S. Casasso, M. Citron, D. Colling, L. Corpe, P. Dauncey, G. Davies, A. De Wit, M. Della Negra, R. Di Maria, A. Elwood, Y. Haddad, G. Hall, G. Iles, T. James, R. Lane, C. Laner, L. Lyons, A.-M. Magnan,

S. Malik, L. Mastrolorenzo, T. Matsushita, J. Nash, A. Nikitenko[7], V. Palladino, M. Pesaresi, D.M. Raymond, A. Richards, A. Rose, E. Scott, C. Seez, A. Shtipliyski, S. Summers, A. Tapper, K. Uchida, M. Vazquez Acosta[62], T. Virdee[14], N. Wardle, D. Winterbottom, J. Wright, S.C. Zenz

Brunel University, Uxbridge, United Kingdom
J.E. Cole, P.R. Hobson, A. Khan, P. Kyberd, I.D. Reid, L. Teodorescu, M. Turner, S. Zahid

Baylor University, Waco, USA
A. Borzou, K. Call, J. Dittmann, K. Hatakeyama, H. Liu, N. Pastika, C. Smith

Catholic University of America, Washington DC, USA
R. Bartek, A. Dominguez

The University of Alabama, Tuscaloosa, USA
A. Buccilli, S.I. Cooper, C. Henderson, P. Rumerio, C. West

Boston University, Boston, USA
D. Arcaro, A. Avetisyan, T. Bose, D. Gastler, D. Rankin, C. Richardson, J. Rohlf, L. Sulak, D. Zou

Brown University, Providence, USA
G. Benelli, D. Cutts, A. Garabedian, M. Hadley, J. Hakala, U. Heintz, J.M. Hogan, K.H.M. Kwok, E. Laird, G. Landsberg, J. Lee, Z. Mao, M. Narain, J. Pazzini, S. Piperov, S. Sagir, R. Syarif, D. Yu

University of California, Davis, Davis, USA
R. Band, C. Brainerd, R. Breedon, D. Burns, M. Calderon De La Barca Sanchez, M. Chertok, J. Conway, R. Conway, P.T. Cox, R. Erbacher, C. Flores, G. Funk, W. Ko, R. Lander, C. Mclean, M. Mulhearn, D. Pellett, J. Pilot, S. Shalhout, M. Shi, J. Smith, D. Stolp, K. Tos, M. Tripathi, Z. Wang

University of California, Los Angeles, USA
M. Bachtis, C. Bravo, R. Cousins, A. Dasgupta, A. Florent, J. Hauser, M. Ignatenko, N. Mccoll, S. Regnard, D. Saltzberg, C. Schnaible, V. Valuev

University of California, Riverside, Riverside, USA
E. Bouvier, K. Burt, R. Clare, J. Ellison, J.W. Gary, S.M.A. Ghiasi Shirazi, G. Hanson, J. Heilman, G. Karapostoli, E. Kennedy, F. Lacroix, O.R. Long, M. Olmedo Negrete, M.I. Paneva, W. Si, L. Wang, H. Wei, S. Wimpenny, B. R. Yates

University of California, San Diego, La Jolla, USA
J.G. Branson, S. Cittolin, M. Derdzinski, R. Gerosa, D. Gilbert, B. Hashemi, A. Holzner, D. Klein, G. Kole, V. Krutelyov, J. Letts, I. Macneill, M. Masciovecchio, D. Olivito, S. Padhi, M. Pieri, M. Sani, V. Sharma, S. Simon, M. Tadel, A. Vartak, S. Wasserbaech[63], J. Wood, F. Würthwein, A. Yagil, G. Zevi Della Porta

University of California, Santa Barbara - Department of Physics, Santa Barbara, USA
N. Amin, R. Bhandari, J. Bradmiller-Feld, C. Campagnari, A. Dishaw, V. Dutta, M. Franco Sevilla, F. Golf, L. Gouskos, R. Heller, J. Incandela, A. Ovcharova, H. Qu, J. Richman, D. Stuart, I. Suarez, J. Yoo

California Institute of Technology, Pasadena, USA
D. Anderson, A. Bornheim, J.M. Lawhorn, H.B. Newman, T. Nguyen, C. Pena, M. Spiropulu, J.R. Vlimant, S. Xie, Z. Zhang, R.Y. Zhu

Carnegie Mellon University, Pittsburgh, USA
M.B. Andrews, T. Ferguson, T. Mudholkar, M. Paulini, J. Russ, M. Sun, H. Vogel, I. Vorobiev, M. Weinberg

University of Colorado Boulder, Boulder, USA
J.P. Cumalat, W.T. Ford, F. Jensen, A. Johnson, M. Krohn, S. Leontsinis, T. Mulholland, K. Stenson, S.R. Wagner

Cornell University, Ithaca, USA
J. Alexander, J. Chaves, J. Chu, S. Dittmer, K. Mcdermott, N. Mirman, J.R. Patterson, D. Quach, A. Rinkevicius, A. Ryd, L. Skinnari, L. Soffi, S.M. Tan, Z. Tao, J. Thom, J. Tucker, P. Wittich, M. Zientek

Fermi National Accelerator Laboratory, Batavia, USA
S. Abdullin, M. Albrow, M. Alyari, G. Apollinari, A. Apresyan, A. Apyan, S. Banerjee, L.A.T. Bauerdick, A. Beretvas, J. Berryhill, P.C. Bhat, G. Bolla†, K. Burkett, J.N. Butler, A. Canepa, G.B. Cerati, H.W.K. Cheung, F. Chlebana, M. Cremonesi, J. Duarte, V.D. Elvira, J. Freeman, Z. Gecse, E. Gottschalk, L. Gray, D. Green, S. Grünendahl, O. Gutsche, R.M. Harris, S. Hasegawa, J. Hirschauer, Z. Hu, B. Jayatilaka, S. Jindariani, M. Johnson, U. Joshi, B. Klima, B. Kreis, S. Lammel, D. Lincoln, R. Lipton, M. Liu, T. Liu, R. Lopes De Sá, J. Lykken, K. Maeshima, N. Magini, J.M. Marraffino, D. Mason, P. McBride, P. Merkel, S. Mrenna, S. Nahn, V. O'Dell, K. Pedro, O. Prokofyev, G. Rakness, L. Ristori, B. Schneider, E. Sexton-Kennedy, A. Soha, W.J. Spalding, L. Spiegel, S. Stoynev, J. Strait, N. Strobbe, L. Taylor, S. Tkaczyk, N.V. Tran, L. Uplegger, E.W. Vaandering, C. Vernieri, M. Verzocchi, R. Vidal, M. Wang, H.A. Weber, A. Whitbeck

University of Florida, Gainesville, USA
D. Acosta, P. Avery, P. Bortignon, D. Bourilkov, A. Brinkerhoff, A. Carnes, M. Carver, D. Curry, R.D. Field, I.K. Furic, S.V. Gleyzer, B.M. Joshi, J. Konigsberg, A. Korytov, K. Kotov, P. Ma, K. Matchev, H. Mei, G. Mitselmakher, D. Rank, K. Shi, D. Sperka, N. Terentyev, L. Thomas, J. Wang, S. Wang, J. Yelton

Florida International University, Miami, USA
Y.R. Joshi, S. Linn, P. Markowitz, J.L. Rodriguez

Florida State University, Tallahassee, USA
A. Ackert, T. Adams, A. Askew, S. Hagopian, V. Hagopian, K.F. Johnson, T. Kolberg, G. Martinez, T. Perry, H. Prosper, A. Saha, A. Santra, V. Sharma, R. Yohay

Florida Institute of Technology, Melbourne, USA
M.M. Baarmand, V. Bhopatkar, S. Colafranceschi, M. Hohlmann, D. Noonan, T. Roy, F. Yumiceva

University of Illinois at Chicago (UIC), Chicago, USA
M.R. Adams, L. Apanasevich, D. Berry, R.R. Betts, R. Cavanaugh, X. Chen, O. Evdokimov, C.E. Gerber, D.A. Hangal, D.J. Hofman, K. Jung, J. Kamin, I.D. Sandoval Gonzalez, M.B. Tonjes, H. Trauger, N. Varelas, H. Wang, Z. Wu, J. Zhang

The University of Iowa, Iowa City, USA
B. Bilki[64], W. Clarida, K. Dilsiz[65], S. Durgut, R.P. Gandrajula, M. Haytmyradov, V. Khristenko, J.-P. Merlo, H. Mermerkaya[66], A. Mestvirishvili, A. Moeller, J. Nachtman, H. Ogul[67], Y. Onel, F. Ozok[68], A. Penzo, C. Snyder, E. Tiras, J. Wetzel, K. Yi

Johns Hopkins University, Baltimore, USA
B. Blumenfeld, A. Cocoros, N. Eminizer, D. Fehling, L. Feng, A.V. Gritsan, P. Maksimovic, J. Roskes, U. Sarica, M. Swartz, M. Xiao, C. You

The University of Kansas, Lawrence, USA
A. Al-bataineh, P. Baringer, A. Bean, S. Boren, J. Bowen, J. Castle, S. Khalil, A. Kropivnitskaya, D. Majumder, W. Mcbrayer, M. Murray, C. Royon, S. Sanders, E. Schmitz, J.D. Tapia Takaki, Q. Wang

Kansas State University, Manhattan, USA
A. Ivanov, K. Kaadze, Y. Maravin, A. Mohammadi, L.K. Saini, N. Skhirtladze, S. Toda

Lawrence Livermore National Laboratory, Livermore, USA
F. Rebassoo, D. Wright

University of Maryland, College Park, USA
C. Anelli, A. Baden, O. Baron, A. Belloni, S.C. Eno, Y. Feng, C. Ferraioli, N.J. Hadley, S. Jabeen, G.Y. Jeng, R.G. Kellogg, J. Kunkle, A.C. Mignerey, F. Ricci-Tam, Y.H. Shin, A. Skuja, S.C. Tonwar

Massachusetts Institute of Technology, Cambridge, USA
D. Abercrombie, B. Allen, V. Azzolini, R. Barbieri, A. Baty, R. Bi, S. Brandt, W. Busza, I.A. Cali, M. D'Alfonso, Z. Demiragli, G. Gomez Ceballos, M. Goncharov, D. Hsu, M. Hu, Y. Iiyama, G.M. Innocenti, M. Klute, D. Kovalskyi, Y.S. Lai, Y.-J. Lee, A. Levin, P.D. Luckey, B. Maier, A.C. Marini, C. Mcginn, C. Mironov, S. Narayanan, X. Niu, C. Paus, C. Roland, G. Roland, J. Salfeld-Nebgen, G.S.F. Stephans, K. Tatar, D. Velicanu, J. Wang, T.W. Wang, B. Wyslouch

University of Minnesota, Minneapolis, USA
A.C. Benvenuti, R.M. Chatterjee, A. Evans, P. Hansen, J. Hiltbrand, S. Kalafut, Y. Kubota, Z. Lesko, J. Mans, S. Nourbakhsh, N. Ruckstuhl, R. Rusack, J. Turkewitz, M.A. Wadud

University of Mississippi, Oxford, USA
J.G. Acosta, S. Oliveros

University of Nebraska-Lincoln, Lincoln, USA
E. Avdeeva, K. Bloom, D.R. Claes, C. Fangmeier, R. Gonzalez Suarez, R. Kamalieddin, I. Kravchenko, J. Monroy, J.E. Siado, G.R. Snow, B. Stieger

State University of New York at Buffalo, Buffalo, USA
J. Dolen, A. Godshalk, C. Harrington, I. Iashvili, D. Nguyen, A. Parker, S. Rappoccio, B. Roozbahani

Northeastern University, Boston, USA
G. Alverson, E. Barberis, A. Hortiangtham, A. Massironi, D.M. Morse, T. Orimoto, R. Teixeira De Lima, D. Trocino, D. Wood

Northwestern University, Evanston, USA
S. Bhattacharya, O. Charaf, K.A. Hahn, N. Mucia, N. Odell, B. Pollack, M.H. Schmitt, K. Sung, M. Trovato, M. Velasco

University of Notre Dame, Notre Dame, USA
N. Dev, M. Hildreth, K. Hurtado Anampa, C. Jessop, D.J. Karmgard, N. Kellams, K. Lannon, W. Li, N. Loukas, N. Marinelli, F. Meng, C. Mueller, Y. Musienko[35], M. Planer, A. Reinsvold, R. Ruchti, P. Siddireddy, G. Smith, S. Taroni, M. Wayne, A. Wightman, M. Wolf, A. Woodard

The Ohio State University, Columbus, USA
J. Alimena, L. Antonelli, B. Bylsma, L.S. Durkin, S. Flowers, B. Francis, A. Hart, C. Hill, W. Ji, B. Liu, W. Luo, B.L. Winer, H.W. Wulsin

Princeton University, Princeton, USA
S. Cooperstein, O. Driga, P. Elmer, J. Hardenbrook, P. Hebda, S. Higginbotham,

A. Kalogeropoulos, D. Lange, J. Luo, D. Marlow, K. Mei, I. Ojalvo, J. Olsen, C. Palmer, P. Piroué, D. Stickland, C. Tully

University of Puerto Rico, Mayaguez, USA
S. Malik, S. Norberg

Purdue University, West Lafayette, USA
A. Barker, V.E. Barnes, S. Das, S. Folgueras, L. Gutay, M.K. Jha, M. Jones, A.W. Jung, A. Khatiwada, D.H. Miller, N. Neumeister, C.C. Peng, H. Qiu, J.F. Schulte, J. Sun, F. Wang, W. Xie

Purdue University Northwest, Hammond, USA
T. Cheng, N. Parashar, J. Stupak

Rice University, Houston, USA
A. Adair, Z. Chen, K.M. Ecklund, S. Freed, F.J.M. Geurts, M. Guilbaud, M. Kilpatrick, W. Li, B. Michlin, M. Northup, B.P. Padley, J. Roberts, J. Rorie, W. Shi, Z. Tu, J. Zabel, A. Zhang

University of Rochester, Rochester, USA
A. Bodek, P. de Barbaro, R. Demina, Y.t. Duh, T. Ferbel, M. Galanti, A. Garcia-Bellido, J. Han, O. Hindrichs, A. Khukhunaishvili, K.H. Lo, P. Tan, M. Verzetti

The Rockefeller University, New York, USA
R. Ciesielski, K. Goulianos, C. Mesropian

Rutgers, The State University of New Jersey, Piscataway, USA
A. Agapitos, J.P. Chou, Y. Gershtein, T.A. Gómez Espinosa, E. Halkiadakis, M. Heindl, E. Hughes, S. Kaplan, R. Kunnawalkam Elayavalli, S. Kyriacou, A. Lath, R. Montalvo, K. Nash, M. Osherson, H. Saka, S. Salur, S. Schnetzer, D. Sheffield, S. Somalwar, R. Stone, S. Thomas, P. Thomassen, M. Walker

University of Tennessee, Knoxville, USA
A.G. Delannoy, M. Foerster, J. Heideman, G. Riley, K. Rose, S. Spanier, K. Thapa

Texas A&M University, College Station, USA
O. Bouhali[69], A. Castaneda Hernandez[69], A. Celik, M. Dalchenko, M. De Mattia, A. Delgado, S. Dildick, R. Eusebi, J. Gilmore, T. Huang, T. Kamon[70], R. Mueller, Y. Pakhotin, R. Patel, A. Perloff, L. Perniè, D. Rathjens, A. Safonov, A. Tatarinov, K.A. Ulmer

Texas Tech University, Lubbock, USA
N. Akchurin, J. Damgov, F. De Guio, P.R. Dudero, J. Faulkner, E. Gurpinar, S. Kunori, K. Lamichhane, S.W. Lee, T. Libeiro, T. Mengke, S. Muthumuni, T. Peltola, S. Undleeb, I. Volobouev, Z. Wang

Vanderbilt University, Nashville, USA
S. Greene, A. Gurrola, R. Janjam, W. Johns, C. Maguire, A. Melo, H. Ni, K. Padeken, P. Sheldon, S. Tuo, J. Velkovska, Q. Xu

University of Virginia, Charlottesville, USA
M.W. Arenton, P. Barria, B. Cox, R. Hirosky, M. Joyce, A. Ledovskoy, H. Li, C. Neu, T. Sinthuprasith, Y. Wang, E. Wolfe, F. Xia

Wayne State University, Detroit, USA
R. Harr, P.E. Karchin, N. Poudyal, J. Sturdy, P. Thapa, S. Zaleski

University of Wisconsin - Madison, Madison, WI, USA
M. Brodski, J. Buchanan, C. Caillol, S. Dasu, L. Dodd, S. Duric, B. Gomber, M. Grothe, M. Herndon, A. Hervé, U. Hussain, P. Klabbers, A. Lanaro, A. Levine, K. Long, R. Loveless, T. Ruggles, A. Savin, N. Smith, W.H. Smith, D. Taylor, N. Woods

†: Deceased
1: Also at Vienna University of Technology, Vienna, Austria
2: Also at State Key Laboratory of Nuclear Physics and Technology, Peking University, Beijing, China
3: Also at IRFU, CEA, Université Paris-Saclay, Gif-sur-Yvette, France
4: Also at Universidade Estadual de Campinas, Campinas, Brazil
5: Also at Universidade Federal de Pelotas, Pelotas, Brazil
6: Also at Université Libre de Bruxelles, Bruxelles, Belgium
7: Also at Institute for Theoretical and Experimental Physics, Moscow, Russia
8: Also at Joint Institute for Nuclear Research, Dubna, Russia
9: Now at Ain Shams University, Cairo, Egypt
10: Now at British University in Egypt, Cairo, Egypt
11: Also at Zewail City of Science and Technology, Zewail, Egypt
12: Also at Université de Haute Alsace, Mulhouse, France
13: Also at Skobeltsyn Institute of Nuclear Physics, Lomonosov Moscow State University, Moscow, Russia
14: Also at CERN, European Organization for Nuclear Research, Geneva, Switzerland
15: Also at RWTH Aachen University, III. Physikalisches Institut A, Aachen, Germany
16: Also at University of Hamburg, Hamburg, Germany
17: Also at Brandenburg University of Technology, Cottbus, Germany
18: Also at MTA-ELTE Lendület CMS Particle and Nuclear Physics Group, Eötvös Loránd University, Budapest, Hungary
19: Also at Institute of Nuclear Research ATOMKI, Debrecen, Hungary
20: Also at Institute of Physics, University of Debrecen, Debrecen, Hungary
21: Also at Indian Institute of Technology Bhubaneswar, Bhubaneswar, India
22: Also at Institute of Physics, Bhubaneswar, India
23: Also at University of Visva-Bharati, Santiniketan, India
24: Also at University of Ruhuna, Matara, Sri Lanka
25: Also at Isfahan University of Technology, Isfahan, Iran
26: Also at Yazd University, Yazd, Iran
27: Also at Plasma Physics Research Center, Science and Research Branch, Islamic Azad University, Tehran, Iran
28: Also at Università degli Studi di Siena, Siena, Italy
29: Also at INFN Sezione di Milano-Bicocca; Università di Milano-Bicocca, Milano, Italy
30: Also at Purdue University, West Lafayette, USA
31: Also at International Islamic University of Malaysia, Kuala Lumpur, Malaysia
32: Also at Malaysian Nuclear Agency, MOSTI, Kajang, Malaysia
33: Also at Consejo Nacional de Ciencia y Tecnología, Mexico city, Mexico
34: Also at Warsaw University of Technology, Institute of Electronic Systems, Warsaw, Poland
35: Also at Institute for Nuclear Research, Moscow, Russia
36: Now at National Research Nuclear University 'Moscow Engineering Physics Institute' (MEPhI), Moscow, Russia
37: Also at St. Petersburg State Polytechnical University, St. Petersburg, Russia
38: Also at University of Florida, Gainesville, USA
39: Also at P.N. Lebedev Physical Institute, Moscow, Russia

40: Also at California Institute of Technology, Pasadena, USA
41: Also at Budker Institute of Nuclear Physics, Novosibirsk, Russia
42: Also at Faculty of Physics, University of Belgrade, Belgrade, Serbia
43: Also at University of Belgrade, Faculty of Physics and Vinca Institute of Nuclear Sciences, Belgrade, Serbia
44: Also at Scuola Normale e Sezione dell'INFN, Pisa, Italy
45: Also at National and Kapodistrian University of Athens, Athens, Greece
46: Also at Riga Technical University, Riga, Latvia
47: Also at Universität Zürich, Zurich, Switzerland
48: Also at Stefan Meyer Institute for Subatomic Physics (SMI), Vienna, Austria
49: Also at Gaziosmanpasa University, Tokat, Turkey
50: Also at Adiyaman University, Adiyaman, Turkey
51: Also at Istanbul Aydin University, Istanbul, Turkey
52: Also at Mersin University, Mersin, Turkey
53: Also at Cag University, Mersin, Turkey
54: Also at Piri Reis University, Istanbul, Turkey
55: Also at Izmir Institute of Technology, Izmir, Turkey
56: Also at Necmettin Erbakan University, Konya, Turkey
57: Also at Marmara University, Istanbul, Turkey
58: Also at Kafkas University, Kars, Turkey
59: Also at Istanbul Bilgi University, Istanbul, Turkey
60: Also at Rutherford Appleton Laboratory, Didcot, United Kingdom
61: Also at School of Physics and Astronomy, University of Southampton, Southampton, United Kingdom
62: Also at Instituto de Astrofísica de Canarias, La Laguna, Spain
63: Also at Utah Valley University, Orem, USA
64: Also at Beykent University, Istanbul, Turkey
65: Also at Bingol University, Bingol, Turkey
66: Also at Erzincan University, Erzincan, Turkey
67: Also at Sinop University, Sinop, Turkey
68: Also at Mimar Sinan University, Istanbul, Istanbul, Turkey
69: Also at Texas A&M University at Qatar, Doha, Qatar
70: Also at Kyungpook National University, Daegu, Korea